# A PHENOMENOLOGICAL APPROACH
# TO STRESS CORROSION CRACKING

by

Mehmet Aydemir NEHROZOĞLU

B.S. in M.E., Boğaziçi University, 1984

Submitted to the Institute for Graduate Studies in

Science and Engineering in Partial Fulfillment of

the requirements for the degree of

Master of Science
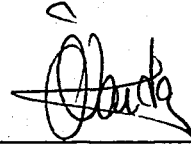
in

Mechanical Engineering

Boğaziçi University

1986

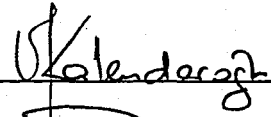# A PHENOMENOLOGICAL APPROACH
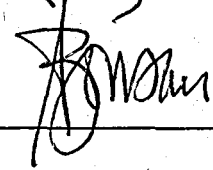# TO STRESS CORROSION CRACKING

APPROVED BY

Doç.Dr.Öktem VARDAR

(Thesis Advisor)

Y.Doç.Dr.Vahan KALENDEROĞLU

Doç.Dr.İlsen ÖNSAN

Date of Approval : June 27,1986
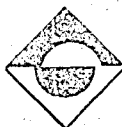
198676

## ACKNOWLEDGEMENTS

# ABSTRACT

The applicability of the J-integral to SSC in the elastic-plastic range is investigated by using precracked cantilever beam specimens of low carbon steel in 6N $H_2SO_4$ solution. The correlation of J-integral with the incubation time suggests the existence of a threshold value of J.

# ÖZET

J-Entegrali'nin elastik-plastik çalışma aralığında GKK'na (Gerilmeli Korozyon Kırılması) uygulanabilirliği araştırıldı. Çalışmada düşük karbonlu çelik'ten ön çatlaklı konsol kiriş numuneler ve korosif olarak 6N $H_2SO_4$ çözeltisi kullanıldı. J-Entegrali ile kuluçka zamanı değerlerinin korrelasyonu J'nin bir eşik değeri olduğunu göstermektedir.

# LIST OF FIGURES

# LIST OF TABLES

# LIST OF CONTENTS

# I. INTRODUCTION

The purpose of this work is to investigate, to an extent, the applicability of the J-integral, developed by Rice, as a parameter controlling the time to failure of components subject to SCC. The successful application of LEFM (Linear elastic fracture mechanics) to SCC in linear elastic conditions has led us to consider and investigate whether the tools of elastic plastic fracture mechanics would, in a similar way, bring simplicity to SCC analysis in the elastic plastic range.

Design oriented researchers have not been interested, as yet, to such an approach and therefore there are very few references (1,2) on this subject. The reasons of this may be summarized as below :

(a) Failure is quite rapid for stress corrosion cracking when stresses reach the yield value. Thus one does never intentionally design to work in this range. At stress levels well below the yield value, which is the usual range of operation, stress intensity factor has been used successfully.

(b) The thicknesses of the components, which SCC problems are confined to, are generally large enough to establish plane-strain linear elastic conditions.

(c) Determination of the J-integral values for different crack configurations is a difficult practice.

Nevertheless, the J-integral has shown promising progress and it is interesting, with an academic point of view, to investigate whether it can also be used in SCC problems.

## II. GENERAL REVIEW OF THE PROBLEM
## OF STRESS CORROSION

2.1 CRACK INITIATION VS. CRACK PROPAGATION

SCC has been analysed in two distinct phases, namely; crack initiation, and crack propagation. This distinction is similar to that between safe-life and fail safe analyses in fatigue. While crack initiation studies involve the initiation of a crack on a smooth surface, crack propagation involves a damage tolerant analysis which assumes the presence of pre-existing cracks and uses the tools of fracture mechanics. These two phases are often thought, not as complementary to each other but as two distinct cases and are treated separately. The common practice in crack initiation studies is to define a threshold stress, for a given set of environmental conditions, under which stress corrosion crack initiation does not occur.

The fracture mechanics approach does not take into account that cracks can initiate in the absence of defects and thus failure may occur below the threshold value ($K_{ISCC}$) dictated by fracture mechanics. Therefore fracture mechanics and smooth specimen data must be combined in a composite diagram that

describes the SCC resistance in the presence or absence of a precrack. Such a diagram is shown in Figure 2.1



FIGURE 2.1 Composite diagram (Ref.3)
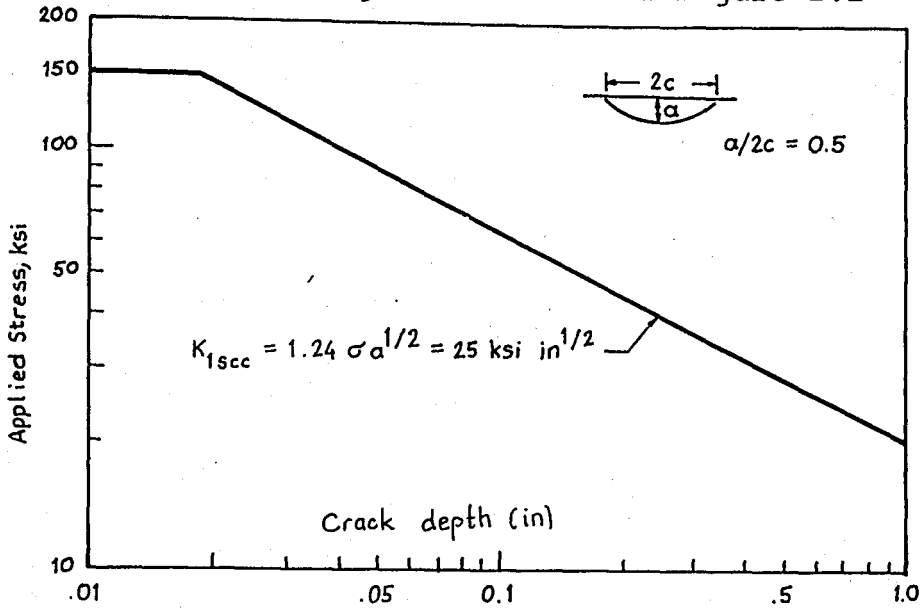
## 2.2 MECHANISMS OF STRESS CORROSION CRACKING

The mechanisms of stress corrosion cracking are not yet fully comprehended. Depending on the material-environment pair and the applied stresses cracking may be intergranular, transgranular or a combination of the two.

Logan(4) has taken up the subject in some detail and has noted the following :

(a) Stress corrosion cracking has one of the characteristics of brittle fracture, it occurs with very little elongation of the material.

(b) Stress corrosion cracking occurs only if there are effective components of tensile stress acting on the structure.

(c) Pure metals are generally considered to be immune to SCC.

(d) The presence of oxygen is necessary for SCC to occur.

(e) A vast majority of authors have accepted that a specific corodent is necessary to produce SCC in a given alloy.

Although not yet universally accepted, it is widely believed that the film rupture/metal dissolution model is basic to SCC in many cases of interest. According to this model the protective film at the crack tip breaks down by the application of stress and an electrochemical current is induced between the crack tip and the surrounding material thus gradually causing the crack to propagate. Garud and Gerber[5] point out that the driving force for the film rupture/metal dissolution process is the strain rate rather than the strain itself, and that even in constant load tests the controlling parameter for SCC appears to be the strain rate due to creep.

Vermilyea and Diegle[6] propose two conditions for strain-enhanced SCC : (1) The mechanism must produce a crack which lengthens much faster than it widens, and (2) each increment of strain must cause sufficient crack advance by corrosion to produce another equal increment of strain. They formulate their first condition as,

$$\frac{\dot{a}}{\dot{\varepsilon}} > 20 \, \rho \tag{1}$$

where $\rho$ is the crack tip radius, while the second condition is closely related to the steepness of the strain gradient in the vicinity of the crack tip. Vermilyea and Diegle further propose

that for these two conditions to be met the ratio of the crack

tip corrosion rate to the crack tip strain rate must exceed a

critical value in the range of $2.10^{-7}$ cm to $10^{-5}$ cm depending

on the strain gradient ahead of the crack tip.

Herbsleb and Schwenk[7] state that "the importance of

strain rate has implications not only for the evaluation of

in-service parameters but also for establishing the guidelines

for laboratory testing. In relation to the latter there is

strong tendency to keep all of the influencing factors as

constant as possible except for those being investigated.For

this reason the SCC susceptibility of a given system (material

and corrodent constitute a corrosion system) may remain unno-

ticed if the strain rate happens to be below a critical value

$\dot{\varepsilon}_1$ (see Figure 2.2)"
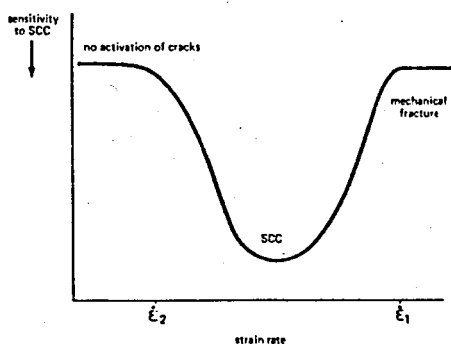


*FIGURE 2.2 Influence of strain rate on sensitivity to SCC (Ref.7)*

# III. APPLICATION OF FRACTURE MECHANICS
# TO SCC

## 3.1 THE STRESS INTENSITY FACTOR APPROACH

The idea of finding a threshold stress intensity factor under which stress corrosion crack propagation does not occur has been the subject of many researches. Rolfe and Barsom[8] have resumed the findings of significant researches on this field. It was observed that similar to the plane strain critical stress intensity factor $K_{IC}$, there exists a threshold stress intensity factor $K_{ISCC}$, which is a property of the material-corrodent system. As long as plane-strain linear elastic conditions prevail $K_{ISCC}$ remains independent of specimen geometry and crack configuration. Many test methods have been devised[9,10,11] in an attempt to determine $K_{ISCC}$. In $K_{ISCC}$ tests the specimens are loaded to an initial stress intensity factor$(K_i)$ and the variation of K with time is observed. Figure 3.1(a) and Figure 3.1(b) show the variation of K as time progresses for constant load and constant displacement tests respectfully. The stress intensity factor increases with time for constant load tests and decreases with time for constant displacement tests. The

time corresponding to the points at which the stress intensity factor starts to increase or decrease depending on the type of test, is the incubation time. While for constant displacement tests crack propagation stops when the stress intensity factor decreases to its threshold value, for constant load tests the increase in K continues until mechanical failure occurs. Figure 3.1(c) shows the variation of the incubation time $t_{inc}$. and time to failure, $t_f$ with K.
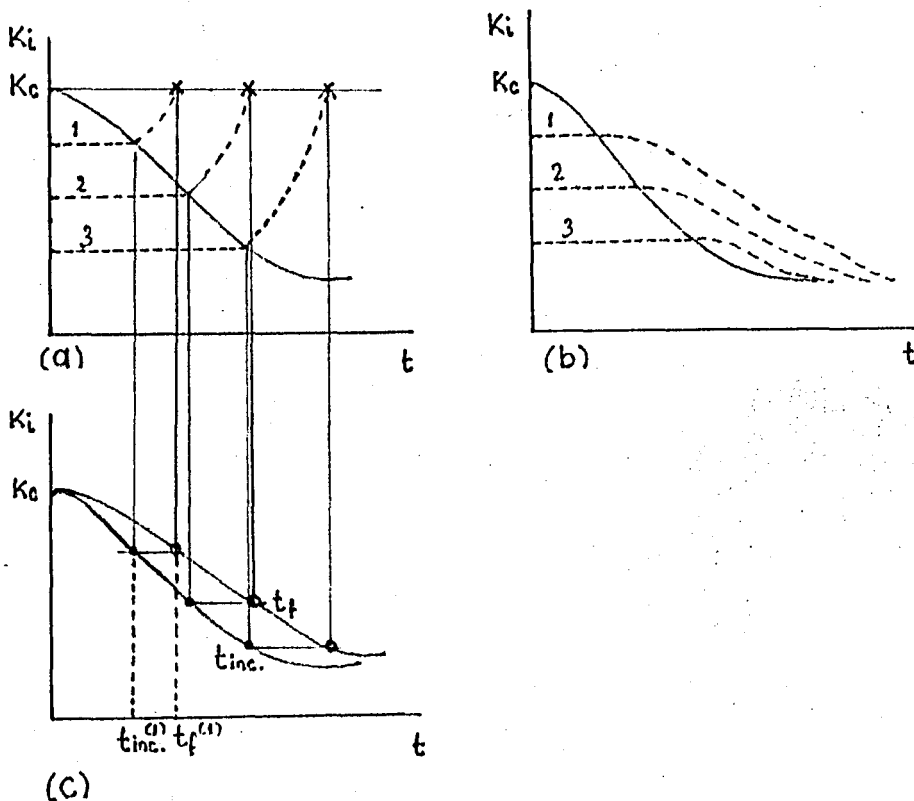
FIGURE 3.1 Variation of K with $t_{inc}$ for
(a) constant load tests,
(b) constant displacement tests and
(c) $t_{inc}$ and $t_f$ as a function of K

The stress intensity factor approach is attractive for
design engineers because of the simplicity of the analysis.
For this reason several attempts have been made recently to
extend the analysis to non plane strain conditions. Novak[12]
has worked on the SCC of ASTM A36, A572 and A517 Grade F
structural steels in salt water. He classified threshold
stress intensity factors for three distinct behaviours as
$K_{ISCC}$, refering to elastic behaviour, "$K_{ISCC}$", refering to
elastic plastic behaviour, and "$K_{ISCC}*$" refering to fully
plastic behaviour. His results showed that the threshold
stress intensity factor for elastic plastic behaviour was
"somewhat dependent" on geometry and therefore had "mixed
validity" as a parameter expressing the crack tip stress-
strain fields, and that for fully plastic behaviour was "fully
dependent" on geometry and was "100% invalid". Another recent
attempt was to define an effective crack length $a_e$, which
is equal to the actual crack length a, plus the radius, $r_y$,
of the plastic zone. Namely;

$$a_e = a + r_y$$

$$r_y = \beta \frac{K^2}{S_y} \qquad (2)$$

$$\beta = \frac{1}{2\pi} \text{ for plane stress}$$

$$\beta = \frac{1}{6\pi} \text{ for plane strain}$$

where $S_y$ is the yield strength. To what extent this approximation has been successful is not stated.

## 3.2 THE J-INTEGRAL APPROACH

### 3.2.1 General

The attempts to find a single parameter capable of characterizing the entire crack tip field under elastic plastic conditions has lead to the development of the J-integral, the general definition of which is given by[14]

$$J = \int_{\Gamma} (Wn_1 - \sigma_{ij} \, n_j \, u_{i,1}) \, ds \qquad (3)$$

where W is the strain energy density and is a function of the strain, n is the outward unit normal to a contour $\Gamma$, encircling the tip of the crack in a counterclockwise direction, and $\ddot{u}_i$ is the displacement vector. The J-integral has been proved to be path-independent, if deformation theory of plasticity is assumed.

The alternative definition of J is expressed by[15]

$$J = - \frac{1}{B} \frac{dU}{da} \bigg|_{\Delta = const.} \qquad (4)$$

where U is the potential energy, B is the thickness of the specimen, a is the crack length and $\Delta$ is the load-line displacement. It can be shown that for the elastic case J is equal to the energy release rate G.

Liu and Zhuang[16] have pointed out that in order for
a single parameter to be capable of characterizing the entire
crack tip field, the plots of any component of $\sigma_{ij}$, $\varepsilon_{ij}$ or
$u_i$ in a given direction versus the distance from the crack
tip r, normalized by $r_y$ $\Delta$, or (J/Sy) should fall on the same
curve for all geometries. The plots of Figure 3.2 show that
single parameter characterization is indeed possible for plane
stress conditions. All of the curves for four different speci-
men geometries fall on top of each other. That is to say, at
any given J value, the crack tip fields in these four different
specimen geometries are the same. While this promising obser-
vation makes way for further research on the J-integral, it is
not yet possible to say whether J characterization will still
be independent of geometry when a corroding environment is
introduced. Another question, as far as SCC is concerned, is
whether a threshold value of J, namely $J_{ISCC}$, exists in a
manner similar to $K_{ISCC}$. If both of the above requirements are
met, the J-integral can be used as a governing parameter in
SCC analysis. References (14-20) provide fundamental information
about elastic - plastic fracture mechanics and the J-integral.
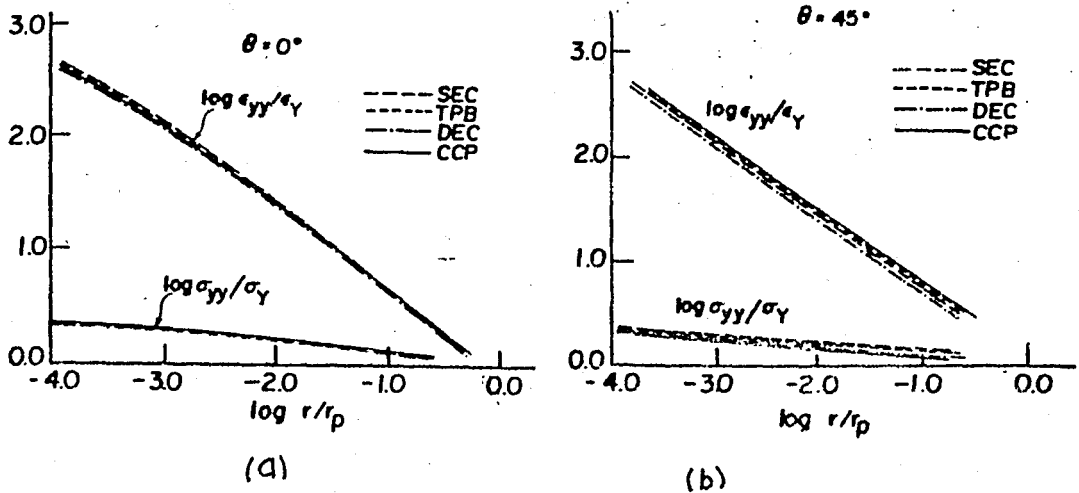
FIGURE 3.2  $\sigma_{yy}$ and $\varepsilon_{yy}$ plane stress characteristic crack tip fields
of all four types of specimen geometries : Single Edge
Cracked, Three Point Bend, Double Edge Cracked, and
Center Cracked Panel.
HY - 80 steel
(a) $\theta = 0$ deg
(b) $\theta = 45$ deg.
(Ref 16)

## 3.2.2 Empirical  Determination of J.

The most suitable expresion for the empirical determination

of J, proposed by Rice-et al, is based on eq.(4). This expression,

developed specifically for deeply cracked bars in bending, is as

follows;

$$J = \frac{2Uc}{Bb} \qquad (5)$$

where $U_c$ is the total energy $U_T$, minus the energy $U_{nc}$ that would

normally exist in the specimen if the specimen did not have a

crack, B is the thickness, and b is the uncracked ligament.

Srawley [21] points out that the error in eq. (5) increases

as a/w decreases and converges to zero as a/w approaches one,

while the use of total energy $U_T$ instead of $U_C$ provides a faster

convergence to a negligible error (Figure 3.3). Therefore, it is actually more suitable to replace $U_C$ by $U_T$ in eq.(5). Noting that $U_T$ is the area, A, under the load vs. displacement curve of the specimen, eq. (5) can be rearranged as

$$J = \frac{2A}{Bb} \tag{6}$$
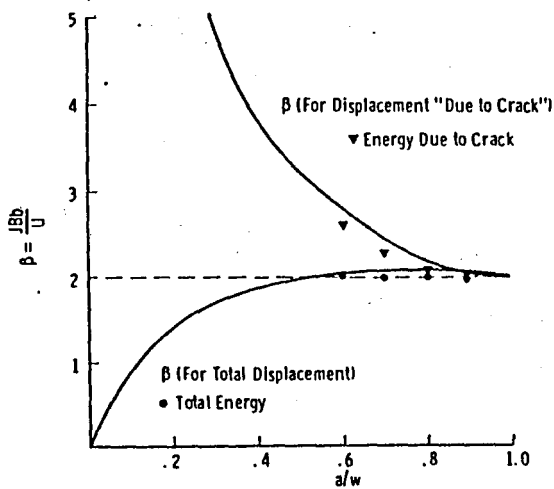


FIGURE 3.3 Values of the nondimensional coefficient β as used in the form J=βU/Bb within the elastic range for a three point bend specimen (Ref.21)

# IV. EXPERIMENTAL WORK

## 4.1 MATERIAL, SPECIMEN AND ENVIRONMENT SELECTION

The material and environment selection in this study was not done to serve a specific application, but rather to provide fully plastic conditions and reasonable experiment times. The material is a low carbon steel with mechanical properties as shown in Table 4.1

TABLE 4.1 *Mechanical Properties of The Low Carbon Steel Used in the Study.*

| Yield (MPa) Strength | Tensile (MPa) Strength | %Elongation |
|---|---|---|
| 250 | 299 | 30 |

6 N. $H_2SO_4$ solution, which is highly agressive to steel is used as the corrodent in order to avoid excessive duration times of experiments.

The specimens are bend type (Figure 4.1) all cut out of

the same plate in the ST orientation.
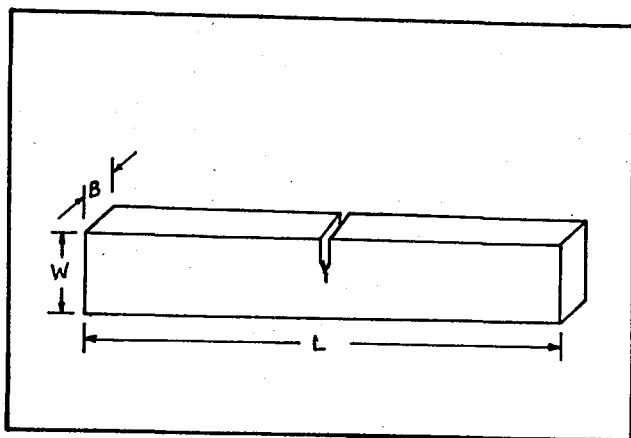


FIGURE 4.1 Details of the bend specimen used in the experiments.
B = 8.5 mm. W = 17 mm, L = 118 mm

## 4.2 EXPERIMENTAL PROCEDURES

The bend type specimens are first precracked in a servo-valve controlled MTS machine in 3-pt bend configuration within a load range of 50-400 kg. The maximum load is set so that large scale plasticity is avoided. A previous study done by A.Koru showed that large scale plasticity caused prolonged incubation times. The 3-pt bend loading configuration is shown in Figure 4.2

(22)
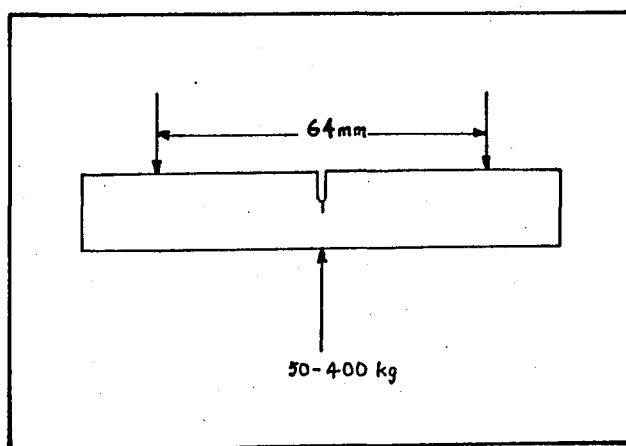


FIGURE 4.2 3-Pt bend loading configuration for fatigue precracking

After precracking the SCC tests are performed on a cantilever beam test set up, shown in Figure 4.3, with the following procedure :

(a) Specimen is mounted and the cup carrying the corrodent is raised so that the specimen is fully embedded in the solution.

(b) Loading is done manually by the application of two kg. and 500 g. weights until the desired load is attanied. Meanwhile the load-line displacement is recorded at each weight addition by use of a dial gage in order to construct the load vs displacement curve.

(c) Displacement vs time data are recorded until a predetermined load-line deflection rate is attained.

(d) After the test the specimens are cooled below their ductile to brittle transition temperature in dry ice and fractured. The initial crack length $a_0$ is measured by use of a travelling microscope (10 X) and the fracture surface is examined to note any evidence of SCC crack growth. If no SCC has taken place the next test is stopped when a higher deflection rate is attained. In this manner the deflection rate at which crack propagation by stress corrosion begins is sought.
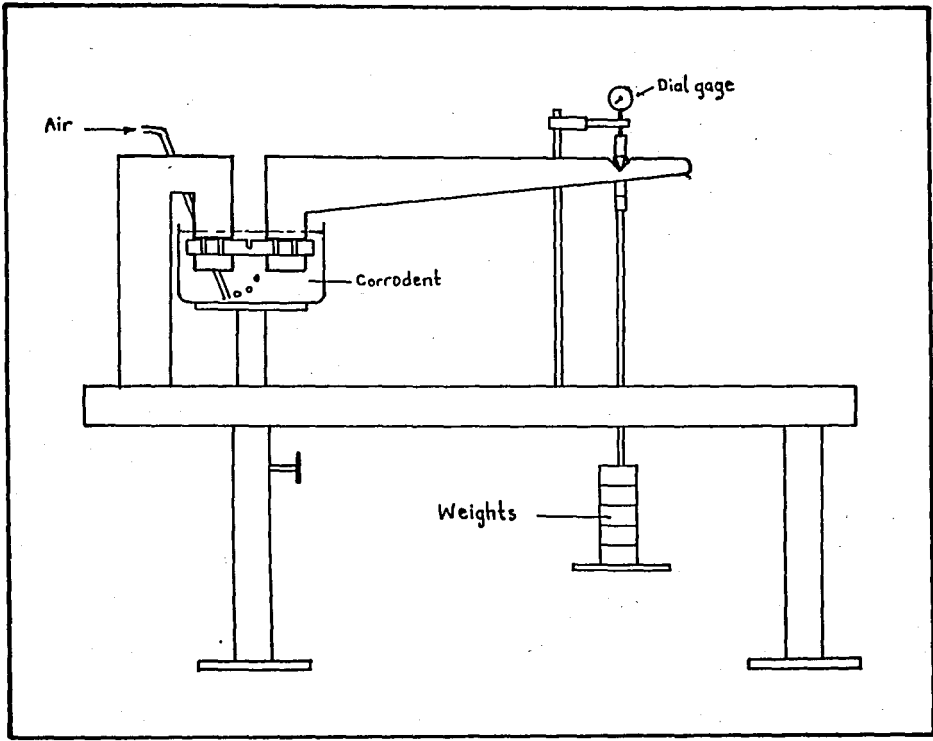
FIGURE 4.3 SCC test set up

# V. RESULTS AND EVALUATION

## 5.1. RÉSUMÉ

Table 5.1 summarizes the outcome of the experiments done
in this study. The controlling parameter for the start of
crack propagation due to stress corrosion is assumed to be the
strain rate and hence the deflection rate. Therefore, the ex-
periments are stopped at various load-line deflection rates in
order to determine at which point of the load-line deflection
vs. time curve the incubation is complete. As seen from Table
5.1 stress corrosion cracks are observed when the experiments
are stopped at a deflection rate value above 0.1 mm/min. It
is observed on a typical deflection vs. time curve, shown in
Figure 5.1 that this point does not correspond, as expected, to
the point where the deflection rate begins to increase above
its steady state value (point P on Figure 5.1). This is indeed
surprizing because any increase of the deflection rate above
its steady state value can only be attributed to crack extension
due to stress corrosion. It can be argued, however, that stress
corrosion cracks do initiate at point p (Figure 5.1) but a cer-
tain time is necessary for these to become through-thickness
cracks. In this study it is assumed that incubation is complete

TABLE 5.1 OUTCOME OF THE SCC EXPERIMENTS

| Specimen | $a_0/W$ | $P_{max}$(kg) | time to conclusion test | deflection rate attained (mm/min) | evidence of SCC |
|---|---|---|---|---|---|
| 12 | 0.41 | 15 | 180 min | $\sim 0.025$ | NO |
| 13 | 0.40 | 14 | 26.75 hrs | $\sim 0.025$ | NO |
| 14 | 0.37 | 14 | 70.50 hrs | $\sim 0.120$ | YES $(\Delta a)_{max}=0.3mm$ |
| 15 1 | 0.42 | 14.5 | 255 min | $\sim 0.07$ | NO |
| 16 | 0.40 | 13.5 | 71 hrs | | NO |
| 18 | 0.39 | 13 | Fractured during loading | | |
| 19 | 0.45 | 14.5 | 36 hrs | $\sim 0.06$ | NO |
| 20 | 0.43 | 14 | 180 min | $\sim 0.06$ | NO |
| 21 | 40 | | | | |
| 22 | 0.44 | 14 | 263 min | $\sim 0.32$ | YES $(\Delta a)_{max} \cong 0.98mm$ |
| 23 | 0.46 | 14.5 | 26.75 hrs | $\sim 0.15$ | YES $(\Delta a)_{max} \cong 0.59mm$ |
| 24 | 0.52 | 13.5 | 10 hrs | $\sim 0.21$ | YES $(\Delta a)_{max} \cong 0.50mm$ |
| 25 | 0.46 | 14 | 245min | $\sim 0.21$ | YES |
| 26 | 0.43 | 13 | 235 min | $\sim 0.24$ | YES $(\Delta a)_{max} \cong 0.59mm$ |

TABLE 5.1 (Cont.)

| Specimen | $a_O/W$ | $P_{max}$(kg) | time to conclusion of test | deflection rate attained (mm/min) | evidence of SCC |
|---|---|---|---|---|---|
| 27 | 0.46 | 12.5 | 30.6 hrs | 0.18 | YES $\Delta a_{max}$=0.59 mm. |
| 28 | 0.43 | 10.5 | 197 hrs conculded beacuse of the bad state of the test set up | $\sim$ 0.022 | NO |
| 30 | 0.42 | 12 | 14.5 hrs | $\sim$0.08 | NO |

only when through cracks appear, therefore the time corres-
ponding to a deflection rate of 0.1 mm/min can be taken as
the incubation time.
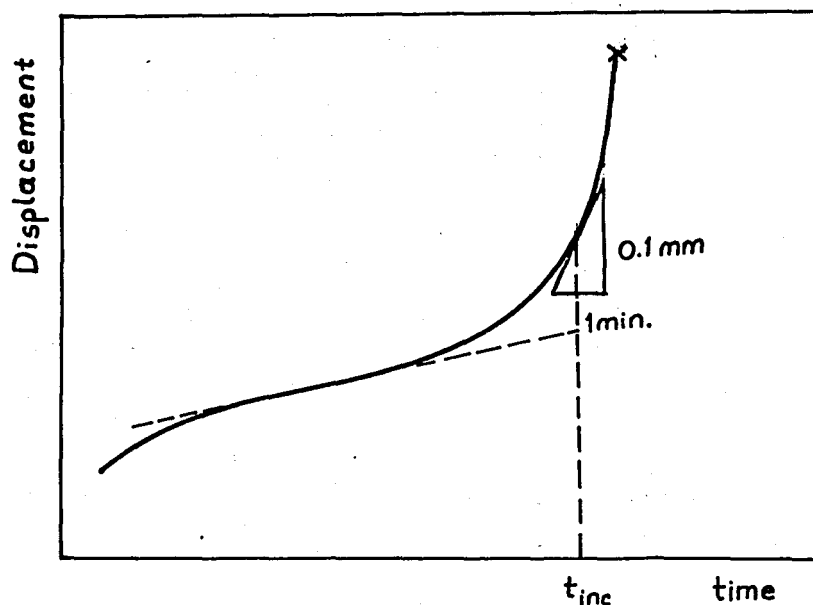


*FIGURE 5.1 Typical Δ-t curve showing the point of incubation*

To be able to use the data of specimens 19 and 20, with
which deflection rate value of 0.06 mm/min was attained,when
plotting the J-integral vs incubation time curve, the incu-
baiton time for all specimens is taken arbitrarily as the time
at which the deflection rate reaches the value 0.06 mm/min.

The data show that the time for the deflection rate to
increase from 0.06 mm/min to 0.1 mm/min is orund 30 minutes
and almost the same for all specimens. Therefore, this choice
of the incubation time is not misleading. Furthermore, the
curvature of the deflection vs. time curves are approximately
the same once the deflection rate is above a value of 0.02 mm/mi

Relying on this observation. the Δ-t curves for specimens
12 and 13, for which the attained deflection rate was around
0.025 mm/min, were extended to the assumed deflection rate
value of 0.06 mm/min to determine their incubation times.

## 5.2 J-INTEGRAL VS. INCUBATION TIME

A typical load vs load-line deflection curve is shown in
Figure 5.2. The area under this curve for each specimen is
determined by use of a planimeter and substituted into eq.
(6) along with the geometric parameters B and b, to determine
the J-integral values. Table 5.2 shows the J-integral and in-
cubation time values for all the specimens. The plot of J-in-
tegral vs. incubation time on linear, semi-log, and log-log
scales are shown in Figures 5.3,5.4, and 5.5 respectively.
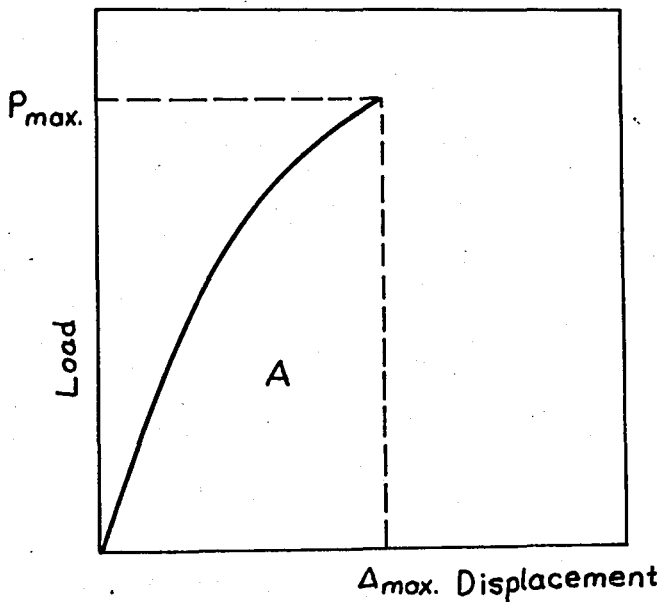


FIGURE 5.2 Typical P-Δ curve

All raw data and graphs obtained from the experiments are
presented in APPENDIX 1.

*TABLE 5.2 J-Integral and Incubation Time Values For the Specimens*

| Specimen | $a_o/W$ * | $P_{max}$ (kg) | J (kg/mm) | $t_{inc}$ ** (min) | log($t_{inc}$) |
|----------|-----------|----------------|-----------|---------------------|----------------|
| 12 | 0.41 | 15 | 1.45 | 210 | 2.32 |
| 13 | 0.40 | 14 | 1.08 | 1610 | 3.21 |
| 14 | 0.37 | 14 | 0.94 | 4200 | 3.62 |
| 15 | 0.42 | 14.5 | too much error in P-Δcurve | 255 | |
| 16 | 0.40 | 13.5 | 0.78 | 4260 *** | 3.63 0 |
| 19 | 0.39 | 14.5 | 1.01 | 2160 | 3.33 |
| 20 | 0.45 | 14 | 1.48 | 180 | 2.25 |
| 22 | 0.43 | 14 | 1.16 | 233 | 2.37 |
| 23 | 0.40 | 14.5 | 1.01 | 1572 | 3.20 |
| 24 | 0.44 | 13.5 | 1.21 | 579 | 2.76 |
| 25 | 0.46 | 14 | 1.21 | 190 | 2.28 |
| 26 | 0.52 | 13 | 1.47 | 175 | 2.24 |
| 27 | 0.46 | 12.5 | 0.89 | 1818 | 3.26 |
| 28 | 0.43 | 10.5 | 0.77 | 11820 *** | 4.07 0 |
| 30 | 0.42 | 12 | 0.64 | 8640 | 3.94 |

* *Bend specimens have W = 17 mm and B =8.5 mm*

** $t_{inc}$ = $t_{0.06}$. $t_{0.06}$ *is the time at which the deflection rate is 0.06 mm/mi*

*** *No Incubation*
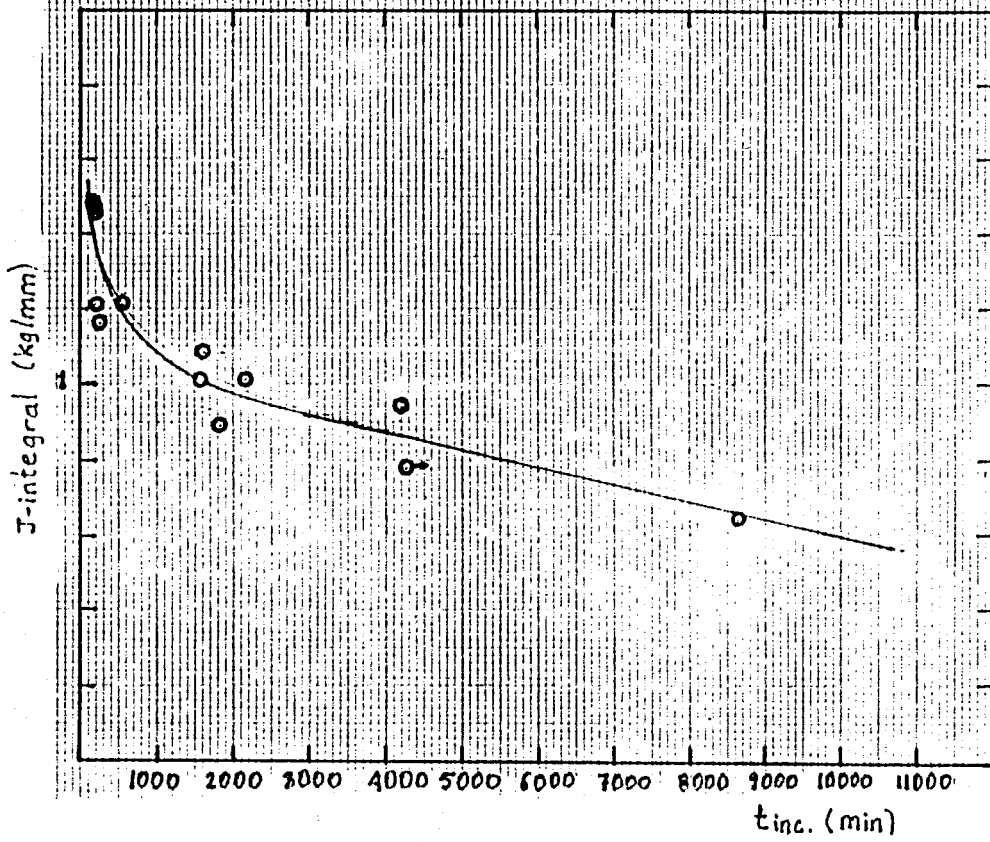
FIGURE 5.3 J-Integral vs. $t_{inc}$ Linear scale
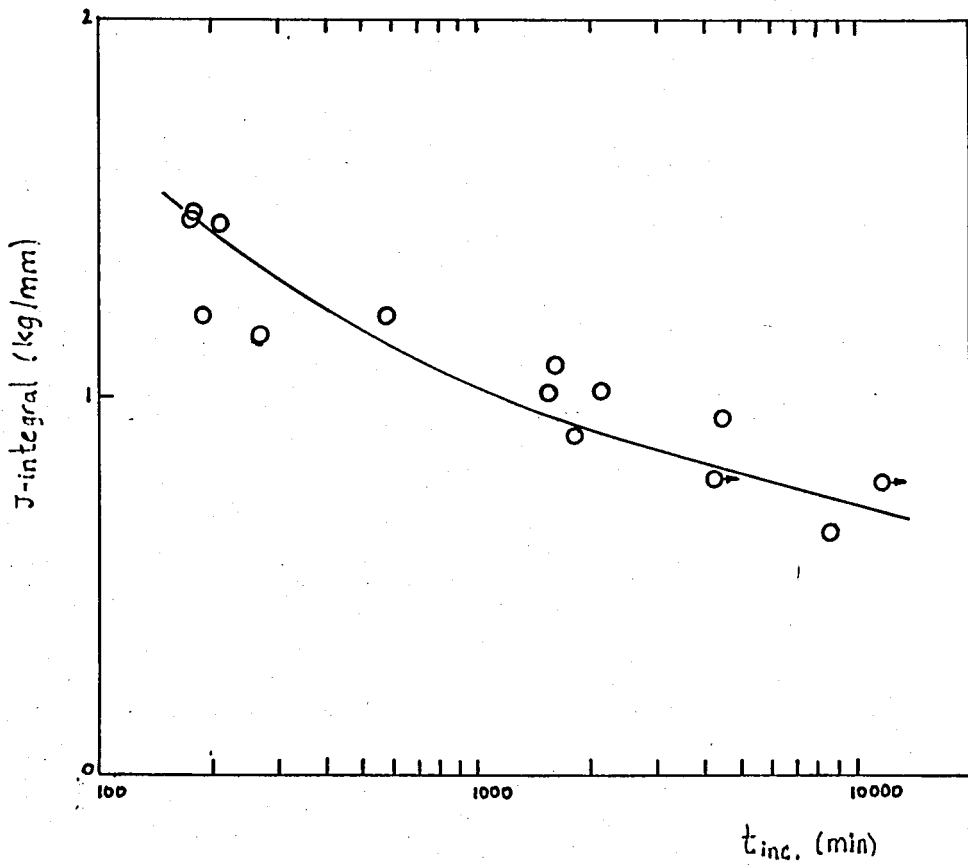


FIGURE 5.4 J-Integral vs. $t_{inc}$ Semi-log scale.

FIGURE 5.5 J-integral vs. tinc log-log scale
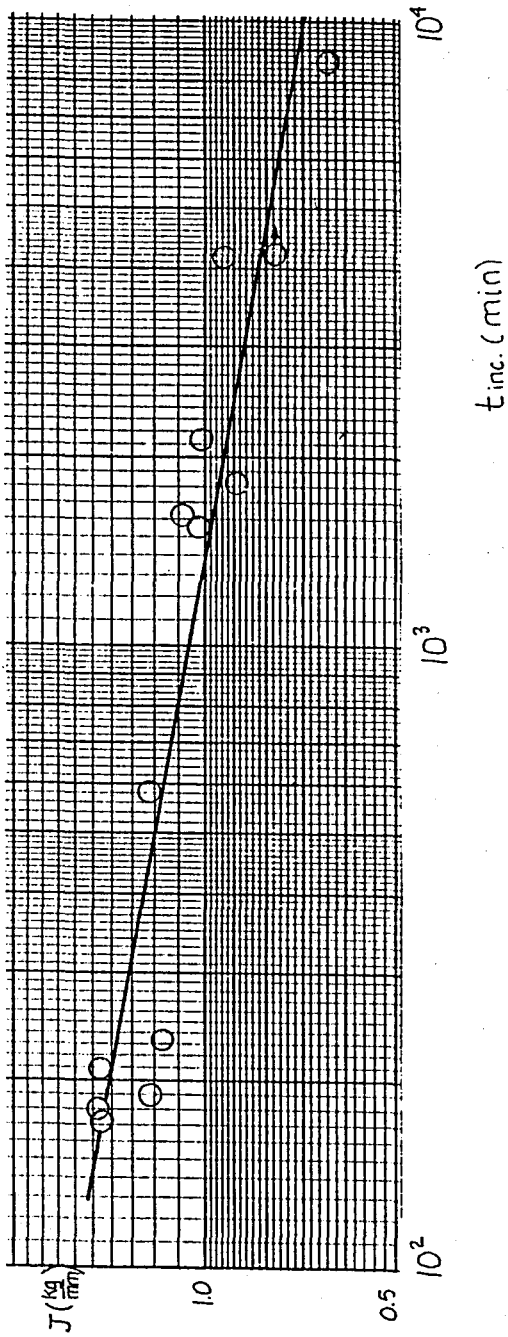
It can be observed from Figs. 5.3 and 5.4 that the curve tends towards a possible threshold. Longer experimental periods lead to excessive deterioration of the specimen due to homogeneous and pitting corrosion. Therefore, the range beyond 10000 min. cannot, unfortunately, be observed.

The low carbon steel used in this study shows extensive creep at room temperature. Especially for specimens with high a/W ratios there is a considerable uncertainty in the load-line displacement readings taken during loading. Table 5.3 compares the J-integral values obtained by taking immediate displacement readings after each weight addition with those obtained by allowing a 30 sec.period after each weight addition before taking the displacement readings. Figures 5.6 and 5.7[23] show the P-Δ curves obtained in this procedure.

TABLE 5.3

| a/W | J-integral immediate reading | (kg/mm) delayed reading | % increase |
|---|---|---|---|
| 0.47 | 1.00 | 1.15 | 15 |
| 0.55 | 1.51 | 1.75 | 16 |
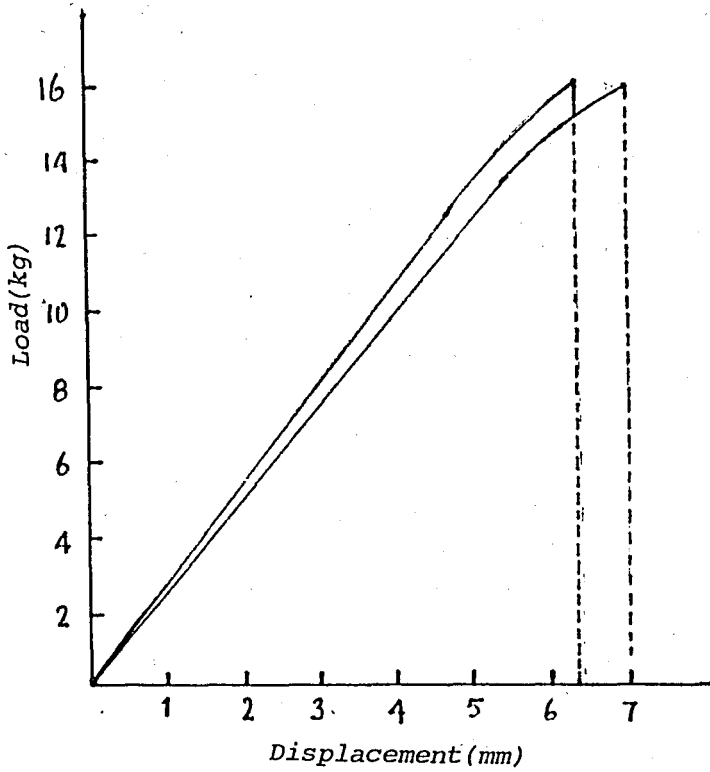
FIGURE 5.6 P-Δ curves showing the creep effect when taking 30 sec.
         delayed deflection readings. a/w = 0.47 (Ref.23)
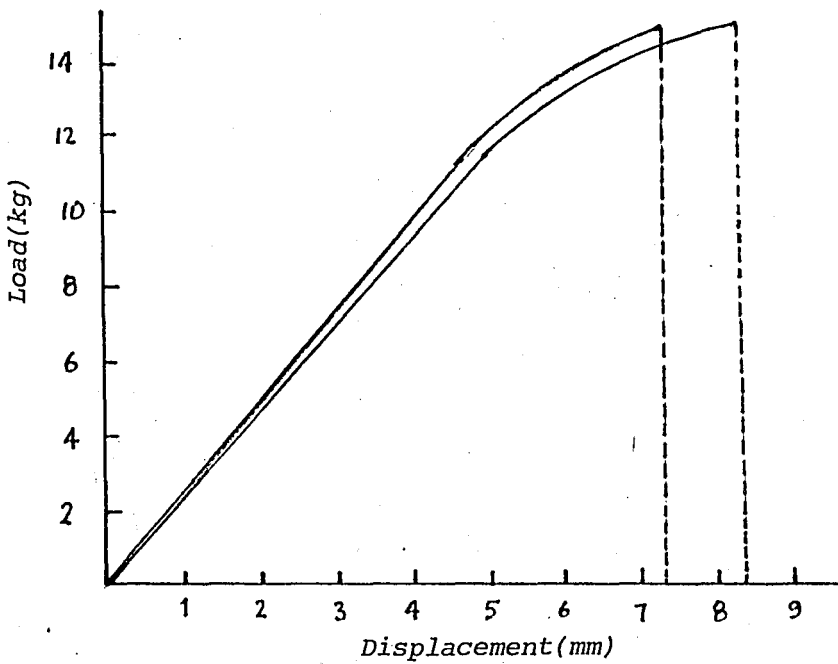


FIGURE 5.7 P - Δ curves showing the creep effect introduced by taking
         30 sec. delayed deflection readings a/w = 0.55 (Ref.23)

Approximately 15% deviation is observed between the
J-integral values found for the two situations. This means
that one could fall into an error at the order of 15% of the
calculated J-integral values. To see amount of error introdu-
ced, the load vs. displacement curves for some of the speci-
mens were reconstructed. First compliance calibration experi-
ments were done and the compliance calibration curve on Figure
5.8 was constructed. Then, four specimens at a/w ratios of 0.38,
0.40, 0.43 and 0.45 were loaded to 15 kg with small weight
increments and meanwhile the deflection readings were taken
immediately after each weight addation. The P-Δ curves for
these four specimens are shown in Figs. A2.1-A2.4. The maximum
displacement $\Delta_{max}$ corresponding to each of the $P_{max}$ values on
Table 5.2 was noted from each of the curves on Figs. A2.1-A2.4.
Figure 5.9 shows the plot of a/w vs. $\Delta_{max}$ at each $P_{max}$ value.
Load vs. displacement curves for those specimens on Table 5.2
with a/w ratios falling between 0.38-0.45 was then replotted
by combining the relevant compliance, $\Delta_{max}$, and $P_{max}$ values.
These plots are shown in Figs.A2.5-8.The new J-integral values
are shown in Table 5.4 and the plot of J-integral vs. incubati-
on time is seen in Figure 5.10. Again the same trend is observed,
and the J-integral values are comparable so it can be concluded
that error due to creep is insignificant within the accuracy of
the test set up.
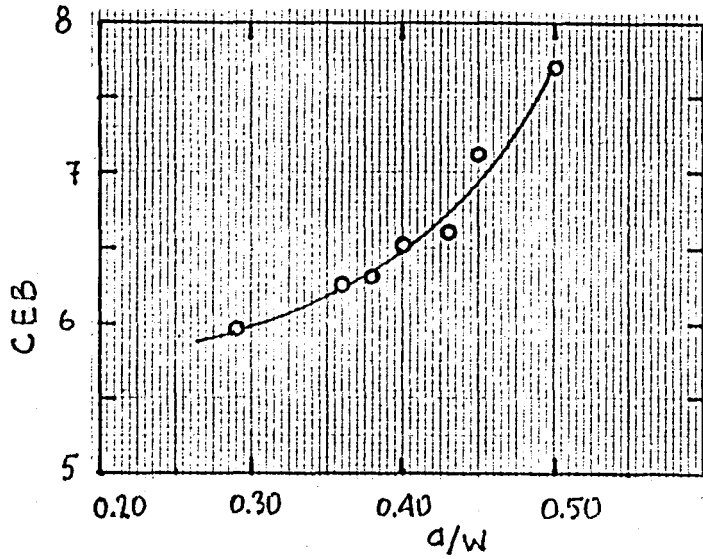
FIGURE 5.8   Compliance calibraiton curve
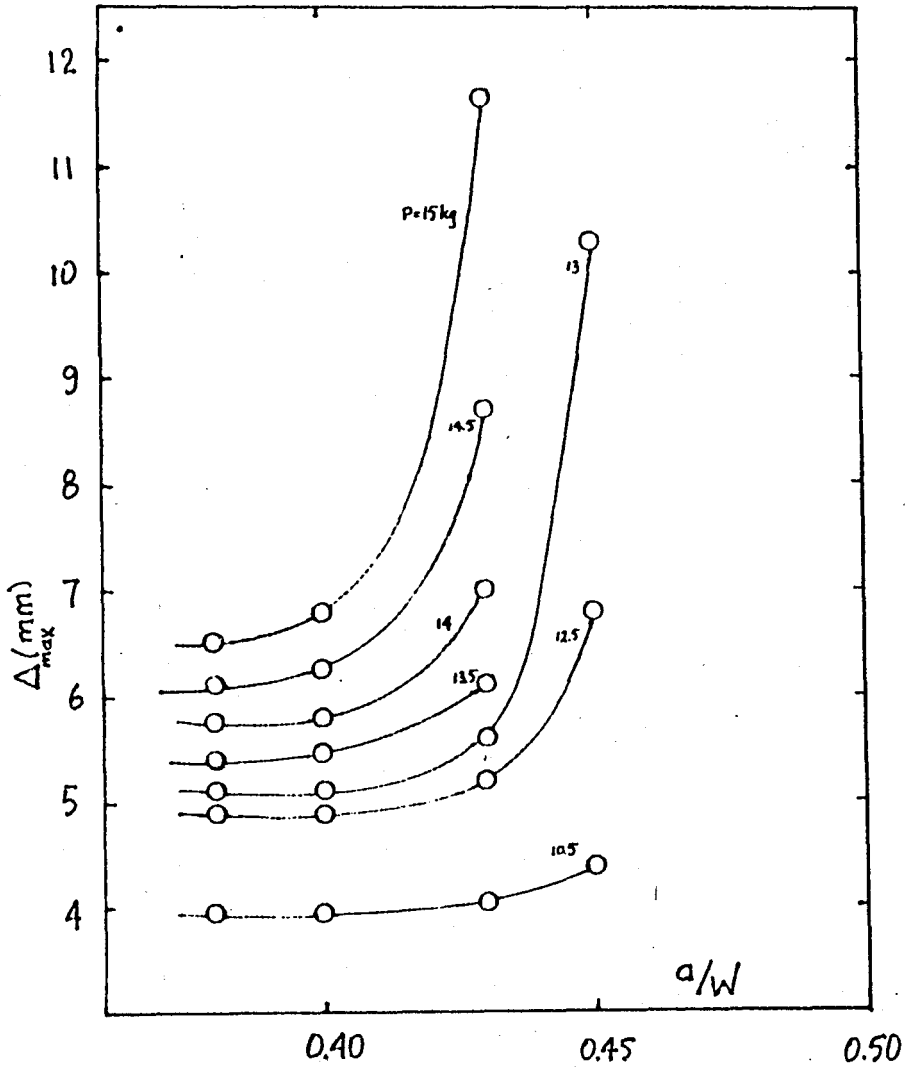


FIGURE 5.9 $\Delta_{max}$ as a function of a/w and $P_{max}$

*TABLE 5.4 J-integral values found from the re-plotted p-Δ curves*

| Spec. | a/W | C(mm/kg) | $\Delta_{max}$(mm) | $P_{max}$(kg) | J (Kg/mm) | $t_{inc}$(min) |
|-------|-----|----------|--------------------|---------------|-----------|----------------|
| 12 | 0.41 | 0.38 | 7.25 | 15 | 1.52 | 210 |
| 13 | 0.40 | 0.38 | 5.80 | 14 | 1.01 | 1610 |
| 14 | 0.37 | 0.36 | 5.70 | 14 | 0.97 | 4200 |
| 15 | 0.42 | 0.39 | 7.15 | 14.5 | 1.40 | 255 |
| 16 | 0.40 | 0.37 | 5.45 | 13.5 | 0.93 | 4260 |
| 19 | 0.39 | 0.37 | 6.05 | 14.5 | 1.07 | 2160 |
| 20 | 0.45 | 0.40 | | 14 | | 180 |
| 22 | 0.43 | 0.40 | 7.00 | 14 | 1.45 | 233 |
| 23 | 0.40 | 0.37 | 6.25 | 14.5 | 1.18 | 1572 |
| 24 | 0.44 | 0.40 | | 13.5 | | 579 |
| 25 | 0.46 | 0.41 | | 14 | | 190 |
| 26 | 0.52 | 0.47 | | 13 | | 175 |
| 27 | 0.46 | 0.41 | 8.75 | 12.5 | | 1818 |
| 28 | 0.43 | 0.40 | 4.05 | 10.5 | 0.53 | 11820 |

All raw data pertaining to this table are presented in APPENDIX-2
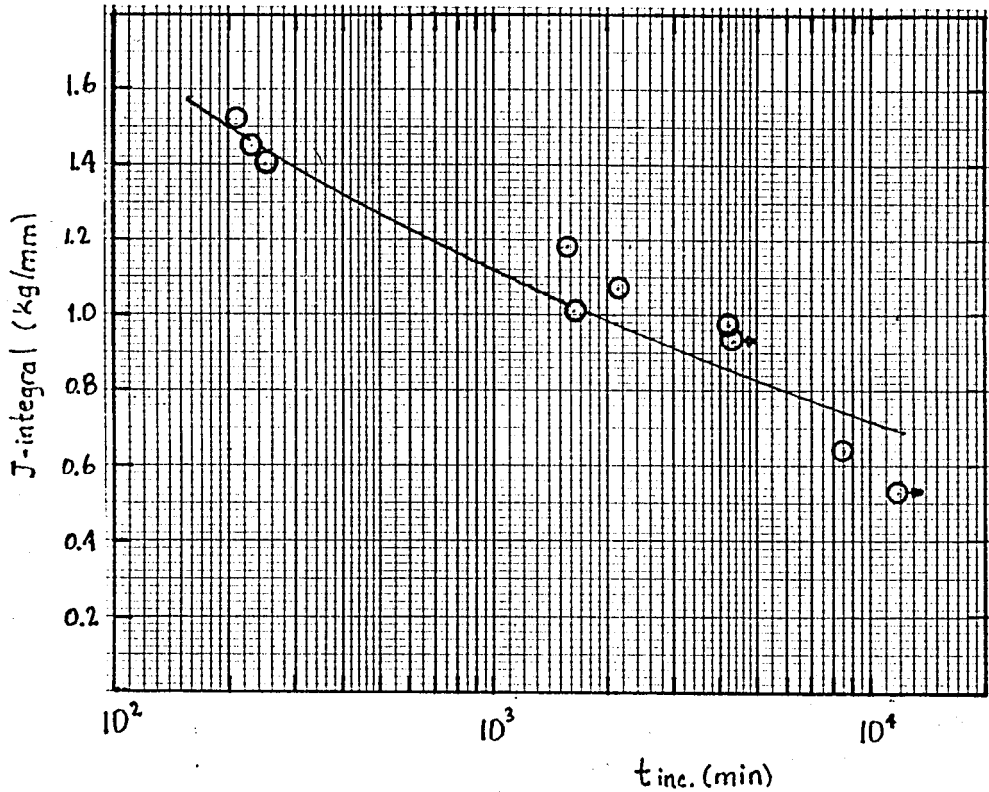
FIGURE 5.10 J-integral vs. incubation time curve with values of
Table 5.4

. . . Another question of interest is how much of the displace-
ment that takes place until the end of the test is due to
creep. Figure 5.11 compares the Δ-t curve of a SCC specimen
with that of a creep specimen, both having the same a/w ratios
and subjected tothe same load. The curvature of both curves is
the same at the initial transient region, while at the steady
state region the deflection rate of the SCC curve is slightly
higher and shows further rapid increase after incubation.
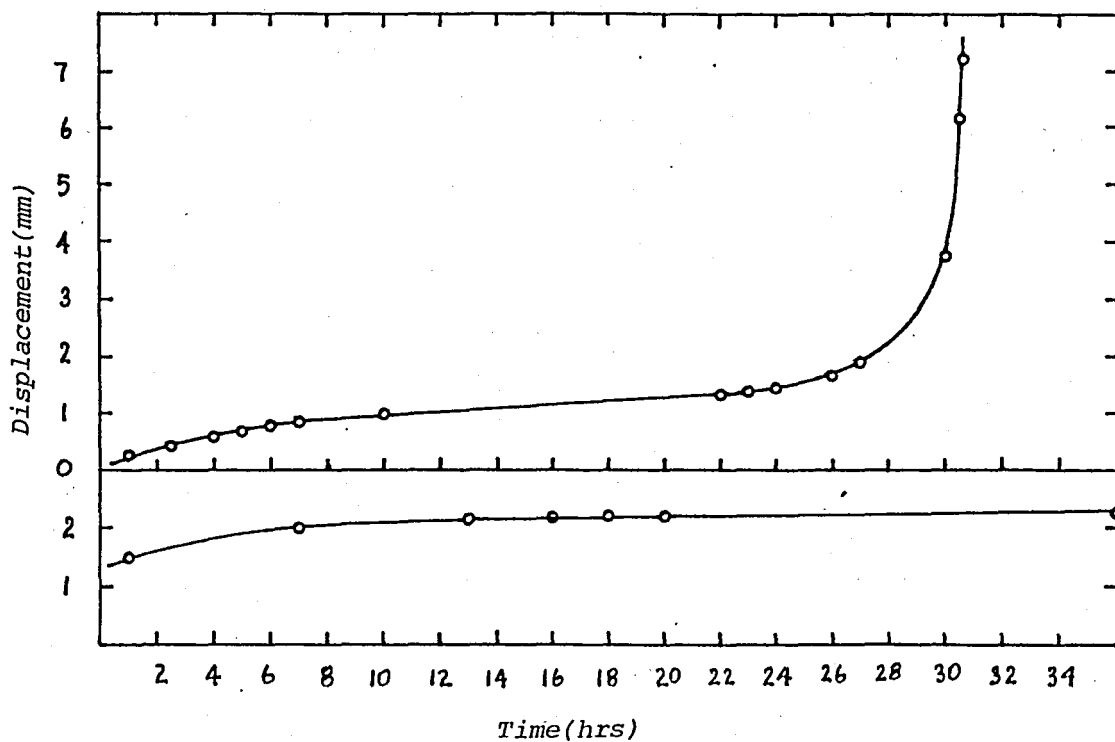
FIGURE 5.11 Δ-t curve of an SCC specimen (top) is compared with that of a creep specimen (bottom). (Both specimens have a/w=0.46 and $P_{max}$=12.5 kg)

## 5.3 CONCLUSIONS

a. The incubation time is controlled by the deflection rate due to creep. The appearance of through cracks are observed when the deflection rate is approximately 0.1 mm/min.

b. The correlation of J-integral with incubation time tends towards a possible threshold. The exact threshold can not be observed because experiment times exceeding $10^4$ min. lead to excessive deterioration of the material due to pitting and homogeneous corrosion.

c. This study was done with a single specimen geometry. Therefore to see whether J-integral characterization is independent from geometry further experimentation is required.

## 5.4 RECOMMENDATIONS

a. It is advisable to do the loading with two persons, one placing the weights and reading the dial gage after each weight is fully applied the other recording the dictated numbers.

b. Sounder data may be obtained by using small weight increments during loading. It is best to start using 500 g. weights after a load of six or at most eight kg. is attained by placing two kg. weights.

c. The best protection of the test set up against acidic solutions is obtained by applying Meges KD 111 coating to the parts of the set up which are directly in contact with the acid. The coating must be checked after each test and must be

replaced after at most 100 hours of operation in the acid.

d. It is necessary to maintain spare bolts and to replace them after at most 100 hours of operation in the acid. It is not necessary to apply coating on the bolts.

e. If possible, it is advisable to keep the acid and prepare the solutions in a separate room. Acid vapor will lead to corrosion of the set up in the long run.

f. Maintaining pieces of cotton cloth and drying the components of the test set up from acid will increase the life of the coating.

# APPENDIX I

## DATA AND CURVES OBTAINED
## FROM THE SCC EXPERIMENTS

*TABLE A1.1 Load vs. Displacement Data for*
   *Spec. 12 (a/w=0.41, $P_{max}$=15 kg)*

| LOAD (kg) | DISPL.(mm) |
|-----------|------------|
| 0 | 0 |
| 3 | 1.05 |
| 5 | 1.75 |
| 7 | 2.58 |
| 9 | 3.49 |
| 11 | 4.42 |
| 13 | 5.56 |
| 15 | Displacement too fast to read |

*TABLE A1.2 Displacement vs. Time data for*
   *spec. 12 (a/w=0.41, $P_{max}$=15 kg)*

| TIME(min) | DISPL.(min) |
|-----------|-------------|
| 0 | 0 |
| 15 | 0.86 |
| 30 | 1.19 |
| 45 | 1.28 |
| 60 | 1.51 |
| 75 | 1.65 |
| 90 | 1.80 |
| 105 | 1.96 |
| 120 | 2.12 |
| 135 | 2.31 |
| 150 | 2.52 |
| 165 | 2.77 |
| 180 | 3.11 |

TABLE A1.3 *Load vs. Displacement data for spec.*
   *13 (a/w=0.40, $P_{max}$ =14 kg)*

| LOAD (kg) | DISPL.(mm) |
|---|---|
| 0 | 0 |
| 3 | 0.79 |
| 5 | 1.45 |
| 7 | 2.04 |
| 9 | 2.65 |
| 11 | 3.41 |
| 12 | 3.90 |
| 13 | 4.60 |
| 14 | 5.55 |

TABLE A1.4 *Displacement vs. Time data for spec.*
   *13 (a/w=0.40, $P_{max}$ =14 kg)*

| TIME (hrs) | DISPL.(mm) |
|---|---|
| 0 | 0 |
| 0.5 | 0.54 |
| 1 | 0.67 |
| 1.5 | 0.75 |
| 2 | 0.79 |
| 2.5 | 0.88 |
| 3 | 0.92 |
| 3.5 | 0.96 |
| 4 | 0.99 |
| 4.5 | 0.03 |
| 5 | 1.07 |
| 5.5 | 1.10 |
| 6 | 1.14 |
| 6.5 | 1.16 |

*Continues on the next page*

*TABLE A1.4 (Cont.)*

| TIME (hrs) | DISPL.(mm) |
|---|---|
| 7 | 1.20 |
| 7.5 | 1.22 |
| 8 | 1.24 |
| 8.5 | 1.26 |
| 20.75 | 2.41 |
| 21.25 | 2.44 |
| 21.75 | 2.48 |
| 22.75 | 2.64 |
| 23.25 | 2.73 |
| 23.50 | 2.78 |
| 23.75 | 2.82 |
| 24.25 | 2.92 |
| 24.75 | 3.04 |
| 25.25 | 3.17 |
| 25.75 | 3.37 |
| 26.25 | 3.72 |
| 26.50 | 3.97 |
| 26.75 | 4.35 |

*TABLE A1.5 Load vs. Displacement data for spec.14 ($a/w=0.37, P_{max}=14$ kg)*

| LOAD (kg) | DISPL.(mm) |
|---|---|
| 0 | 0 |
| 3 | 0.85 |
| 5 | 1.45 |
| 7 | 2.00 |
| 9 | 2.67 |
| 11 | 3.52 |
| 12 | 4.10 |
| 13 | 4.60 |
| 14 | 5.22 |

TABLE A1.6 Displacement vs. Time data
for spec. 14(a/w=0.37,
$P_{max}$=14 kg)

(Cont.)

| TIME (hrs) | DISPL. (mm) | TIME (hrs) | DISPL. (mm) |
|------------|-------------|------------|-------------|
| 0          | 0           | 34         | 2.93        |
| 0.5        | 0.27        | 36.5       | 3.15        |
| 1.         | 0.37        | 37         | 3.22        |
| 2          | 0.50        | 46.50      | 4.48        |
| 3          | 0.57        | 47.00      | 4.55        |
| 4          | 0.64        | 47.50      | 4.64        |
| 5          | 0.69        | 58.50      | 4.83        |
| 6          | 0.74        | 49.50      | 5.05        |
| 7          | 0.79        | 50.50      | 5.27        |
| 21.75      | 1.46        | 51.50      | 5.67        |
| 22.50      | 1.51        | 52.50      | 5.99        |
| 23.50      | 1.58        | 53.50      | 6.27        |
| 24.50      | 1.66        | 55         | 6.74        |
| 26         | 1.81        | 56         | 7.14        |
| 26.50      | 1.87        | 57         | 7.71        |
| 27         | 1.93        | 58         | 8.14        |
| 27.50      | 1.99        | 59         | 8.53        |
| 28         | 2.05        | 60.50      | 9.09        |
| 28.50      | 2.11        | 70.50      | 18.74       |
| 29.50      | 2.26        |            |             |
| 30         | 2.33        |            |             |
| 31         | 2.46        |            |             |
| 32         | 2.61        |            |             |
| 33         | 2.78        |            |             |

*TABLE A1.7 Load vs. Displacement data*
*for spec. 15 (a/w=0.42, $P_{max}$=14.5 kg)*

| LOAD (kg) | DISPL.(mm) |
|-----------|------------|
| 0 | 0 |
| 3 | 1.42 |
| 5 | 2.37 |
| 7 | 3.37 |
| 9 | 4.47 |
| 11 | 5.77 |
| 12 | 6.57 |
| 13 | 7.47 |
| 14 | 8.67 |
| 14.5 | 9.87 |

*TABLE A1.8 Displacement vs. Time data for spec.*
*15(a/w=0.42, $P_{max}$=14.5 kg)*

| TIME (min) | DISPL.(mm) |
|------------|------------|
| 0 | 0 |
| 15 | 0.75 |
| 30 | 1.15 |
| 45 | 1.40 |
| 75 | 1.75 |
| 135 | 2.41 |
| 195 | 3.12 |
| 210 | 3.34 |
| 225 | 3.68 |
| 240 | 4.28 |
| 245 | 4.57 |
| 250 | 4.88 |
| 255 | 5.23 |

TABLE A1.9  Load vs. Displacement data for
specimen 16 (a/w=0.40, $P_{max}$=13.5 kg)

| LOAD (kg) | DISPL. (mm) |
|-----------|-------------|
| 0 | 0 |
| 3 | 0.90 |
| 5 | 1.50 |
| 7 | 2.13 |
| 9 | 2.82 |
| 11 | 3.54 |
| 12 | 3.93 |
| 13 | 4.41 |
| 13.5 | 4.65 |

TABLE A1.10 *Displacement vs. Time data for*
*specimen 16(a/w=0.40 $P_{max}$=13.5 kg)*

| TIME (hrs) | DISPL. (mm) | TIME (hrs) | DISPL. (mm) |
|---|---|---|---|
| 0 | 0 | 44 | 7.95 |
| 1 | 0.79 | 45 | 8.20 |
| 3 | 1.17 | 46.5 | 8.82 |
| 4 | 1.28 | 47 | 9.03 |
| 5 | 1.38 | 47.5 | 9.23 |
| 6 | 1.48 | 48 | 9.46 |
| 7 | 1.57 | 48.5 | 9.71 |
| 8 | 1.64 | 49 | 10.02 |
| 13.5 | 1.91 | 49.5 | 10.37 |
| 24.00 | 2.92 | 50 | 10.78 |
| 25 | 3.05 | 50.5 | 11.17 |
| 26 | 3.22 | 51 | 11.57 |
| 27 | 3.41 | 51.5 | 11.97 |
| 28 | 3.59 | 52.25 | 12.45 |
| 29 | 3.78 | 52.5 | 12.61 |
| 30 | 3.99 | 53 | 12.92 |
| 31 | 4.23 | 53.5 | 13.22 |
| 32 | 4.50 | 54 | 13.48 |
| 33 | 4.79 | 54.5 | 13.69 |
| 35 | 5.40 | 55.5 | 14.05 |
| 36 | 5.75 | 56 | 14.19 |
| 37 | 6.10 | 59 | 14.84 |
| 37.5 | 6.26 | 60.6 | 15.13 |
| | | 71 | 16.66 |

TABLE A1.11 *Load vs Displacement*
*for specimen 19*
*(a/w=0.39, $P_{max}$=14.5kg)*

| LOAD(kg) | DISPL.(mm) |
|----------|------------|
| 0 | 0 |
| 3 | 0.75 |
| 5 | 1.25 |
| 7 | 1.73 |
| 9 | 2.32 |
| 11 | 2.86 |
| 12 | 3.35 |
| 13 | 3.87 |
| 14 | 4.62 |
| 14.5 | 5.05 |

TABLE A1.12 *Displacement vs Time*
*data for spec. 19*
*(a/w=0.39, $P_{max}$=14.5kg)*

| TIME (hrs) | DISPL.(mm) |
|------------|------------|
| 0 | 0 |
| 1 | 0.27 |
| 2 | 0.40 |
| 3 | 0.49 |
| 4 | 0.57 |
| 6 | 0.70 |
| 7.5 | 0.76 |
| 8 | 0.78 |
| 22 | 1.12 |
| 23 | 1.14 |
| 24 | 1.17 |
| 25 | 1.20 |
| 26 | 1.23 |
| 27 | 1.26 |
| 29 | 1.35 |
| 30 | 1.40 |
| 31 | 1.45 |
| 32 | 1.54 |
| 33 | 1.63 |
| 35.5/6 | 3.82 |

TABLE A1.13 Load vs Displacement data for
         Spec. 20 (a/w=0.45, $P_{max}$=14 kg)

| LOAD (kg) | DISPL.(mm) |
|-----------|------------|
| 0 | 0 |
| 3 | 1.13 |
| 5 | 1.88 |
| 7 | 2.63 |
| 9 | 3.43 |
| 11 | 4.31 |
| 13 | 5.55 |
| 14 | 6.85 |

TABLE A1.14 Displacement vs Time data for
         Spec. 20 (a/w=0.45, $P_{max}$=14 kg)

| TIME (min) | DISPL.(mm) |
|------------|------------|
| 0 | 0 |
| 60 | 1.08 |
| 90 | 1.35 |
| 120 | 1.76 |
| 150 | 2.43 |
| 165 | 2.97 |
| 170 | 3.22 |
| 175 | 3.48 |
| 180 | 3.77 |

TABLE A1.15 Load vs. Displ. data
for spec. 22
$(a/w = 0.43, P_{max} = 14 kg)$

TABLE A1.16 Displacement vs Time
data for spec.22
$(a/w = 0.43, P_{max} = 14 kg)$

| LOAD (kg) | DISPL.(mm) | TIME (min) | DISPL.(mm) |
|---|---|---|---|
| 0 | 0 | 0 | 0 |
| 3 | 0.83 | 5 | 0.63 |
| | 1.38 | 10 | 0.86 |
| 7 | 2.01 | 15 | 0.98 |
| 9 | 2.91 | 30 | 1.25 |
| 11 | 3.76 | 45 | 1.48 |
| 13 | 4.96 | 60 | 1.73 |
| 14 | Displacement too fast to read | 75 | 2.01 |
| | | 90 | 2.37 |
| | | 130 | 3.60 |
| | | 135 | 3.77 |
| | | 160 | 4.73 |
| | | 165 | 4.93 |
| | | 180 | 5.57 |
| | | 195 | 6.22 |
| | | 210 | 2.07 |
| | | 230 | 8.23 |
| | | 240 | 8.97 |
| | | 255 | 10.82 |
| | | 260 | 11.95 |
| | | 263 | 12.91 |

TABLE A1.17 Load vs. Displacement data for spec. 23 (a/w=0.40, $P_{max}$=14.5 kg)

| LOAD (kg) | DISPL. (mm) |
|-----------|-------------|
| 0 | 0 |
| 3 | 0.89 |
| 5 | 1.48 |
| 7 | 2.10 |
| 9 | 2.79 |
| 11 | 3.55 |
| 12 | 3.96 |
| 13 | 4.43 |
| 14 | 4.96 |
| 14.5 | 5.36 |

TABLE A1.18 Displacement vs Time data for spec. 23 (a/w=0.40, $P_{max}$=14.5 kg)

| TIME (hrs) | DISPL (mm) |
|------------|------------|
| 0 | 0 |
| 1. | 0.35 |
| 2 | 0.48 |
| 3. | 0.61 |
| 4.5 | 0.77 |
| 5 | 0.82 |
| 55 | 0.86 |
| 6 | 0.90 |
| 7. | 0.96 |
| 8 | 1.01 |
| 9.5 | 1.08 |
| 10 | 1.11 |
| 22 | 1.64 |
| 23 | 1.74 |
| 24 | 1.88 |
| 25 | 2.12 |
| 26 | 2.69 |
| 26.75 | 8.63 |

TABLE A1.19 Load vs Displacement data for spec. 24 $(a/w=0.44, P_{max}=13.5kg)$

| LOAD (kg) | DISPL (mm) |
|-----------|-----------|
| 0 | 0 |
| 3 | 1.02 |
| 5 | 1.70 |
| 7 | 2.45 |
| 9 | 3.27 |
| 11 | 4.12 |
| 12 | 4.68 |
| 13 | 5.53 |
| 13.5 | 6.13 |

TABLE A1.20 Displacement vs. Time data for spec. 24 $(a/w=0.44, P_{max}=13.5 kg)$

| TIME(hrs) | DISPL. (mm) |
|-----------|-------------|
| 0 | 0 |
| 1 | 0.41 |
| 2 | 0.61 |
| 3 | 0.75 |
| 4 | 0.89 |
| 5 | 1.04 |
| 6 | 1.31 |
| 6.5 | 1.51 |
| 7 | 1.79 |
| 7.5 | 2.04 |
| 8 | 2.30 |
| 8.5 | 2.62 |
| 9 | 3.27 |
| 9.5 | 4.48 |
| 10 | 7.08 |

*TABLE A1.21 Load vs Displacement data for spec. 25 ($a/w=0.46$, $P_{max}=14$ kg)*

| LOAD (kg) | DISPL. (mm) |
|-----------|-------------|
| 0         | 0           |
| 3         | 0.78        |
| 5         | 1.30        |
| 7         | 1.97        |
| 9         | 2.62        |
| 11        | 3.37        |
| 13        | 4.47        |
| 14        | 5.47        |

*TABLE A1.22 Displacement vs Time data for spec. 25 ($a/w=0.46$, $P_{max}=14$ kg)*

| TIME (min) | DISPL (min) |
|------------|-------------|
| 0          | 0           |
| 15         | 0.24        |
| 30         | 0.36        |
| 60         | 0.58        |
| 90         | 0.88        |
| 120        | 1.23        |
| 150        | 1.83        |
| 180        | 2.96        |
| 185        | 3.23        |
| 190        | 3.52        |
| 195        | 3.85        |
| 200        | 4.19        |
| 205        | 4.53        |
| 210        | 4.98        |
| 215        | 5.54        |
| 220        | 6.10        |
| 225        | 6.69        |
| 235        | 7.85        |
| 240        | 8.66        |
| 245        | 9.54        |

TABLE A1.23 Load vs Displacement data for spec. 26(a/w=0.52, $P_{max}$=13 kg)

| LOAD (kg) | DISPL. (mm) |
|---|---|
| 0 | 0 |
| 3 | 1.04 |
| 5 | 1.73 |
| 7 | 2.53 |
| 9 | 3.37 |
| 11 | 4.26 |
| 12 | 4.91 |
| 13 | 6.35 |

TABLE A1.24 Displacement vs Time data for spec. 26 (a/w=0.52, $P_{max}$=13 kg)

| TIME(min) | DISPL(mm) |
|---|---|
| 0 | 0 |
| 5 | 0.76 |
| 10 | 1.05 |
| 15 | 1.22 |
| 30 | 1.57 |
| 50 | 1.95 |
| 90 | 2.85 |
| 120 | 3.76 |
| 150 | 5.08 |
| 165 | 5.90 |
| 170 | 6.20 |
| 175 | 6.50 |
| 180 | 6.81 |
| 185 | 7.13 |
| 190 | 7.43 |
| 200 | 8.07 |
| 205 | 8.40 |
| 210 | 8.75 |
| 215 | 9.14 |
| 220 | 9.58 |
| 225 | 10.05 |
| 230 | 10.65 |
| 235 | 11.36 |
| 240 | 12.35 |

TABLE A1.25 Load vs Displacement data for spec. 27 (a/w=0.46, $P_{max}$=12.5 kg)

| LOAD (kg) | DISPL. (mm) |
|-----------|-------------|
| 0 | 0 |
| 3 | 1.05 |
| 5 | 1.75 |
| 7 | 2.45 |
| 9 | 3.28 |
| 11 | 4.12 |
| 12 | 4.72 |
| 12.5 | 5.19 |

TABLE A1.26 Displacement vs Time data for spec. 27 (a/w=0.46, $P_{max}$=12.5 kg)

| TIME (hrs) | DISPL. (mm) |
|------------|-------------|
| 0 | 0 |
| 0.5 | 0.20 |
| 1 | 0.26 |
| 2.5 | 0.42 |
| 4 | 0.59 |
| 5 | 0.68 |
| 6 | 0.77 |
| 7 | 0.84 |
| 10 | 0.98 |
| 22 | 1.35 |
| 23 | 1.39 |
| 24 | 1.44 |
| 26 | 1.66 |
| 27 | 1.90 |
| 28.5 | 2.36 |
| 29.5 | 3.01 |
| 30 | 3.73 |
| 30.5 | 6.16 |
| 30.6 | 7.21 |

TABLE A1.27 Load vs Displacement data for spec. 28 (a/w=0.43, $P_{max}$=10.5 kg)

| LOAD (kg) | DISPL.(mm) |
|-----------|------------|
| 0 | 0 |
| 3 | 1.50 |
| 5 | 2.44 |
| 7 | 3.49 |
| 9 | 4.60 |
| 10 | 5.24 |
| 10.5 | 5.59 |

TABLE A1.28 Displacement vs Time data for spec.28 (a/w=0.43, $P_{max}$=10.5kg)

| TIME (hrs) | DISPL(mm) |
|------------|-----------|
| 0 | 0 |
| 1. | 0.43 |
| 2 | 0.56 |
| 3 | 0.64 |
| 4 | 0.71 |
| 5 | 0.77 |
| 6 | 0.82 |
| 7 | 0.87 |
| 8 | 0.90 |
| 23 | 1.24 |
| 24 | 1.26 |
| 26 | 1.29 |
| 27 | 1.39 |
| 28 | 1.33 |
| 30 | 1.36 |
| 32 | 1.39 |
| 35 | 1.41 |
| 47.5 | 1.51 |
| 52 | 1.54 |
| 55 | 1.56 |
| 72 | 1.68 |
| 76 | 1.71 |
| 79 | 1.74 |
| 98 | 1.95 |

*TABLE A1.28 (Cont.)*

| TIME (hrs) | DISPL.(mm) | TIME (hrs) | DISPL.(mm) |
|---|---|---|---|
| 100 | 2.00 | 155 | 10.11 |
| 102 | 2.06 | 166.5 | 10.71 |
| 119 | 3.15 | 167 | 10.73 |
|  |  | 169.5 | 10.80 |
| 121 | 4.17 | 173 | 10.95 |
| 121.5 | 4.35 | 176 | 11.21 |
| 122.5 | 4.68 | 178 | 11.44 |
| 123 | 4.81 | 179 | 11.56 |
| 123.5 | 4.96 | 190 | 12.35 |
| 124 | 5.10 | 193.5 | 12.83 |
| 125 | 5.41 | 197 |  |
| 126 | 5.75 |  |  |
| 127 | 6.07 |  |  |
| 127.5 | 6.23 |  |  |
| 128 | 6.37 |  |  |
| 129 | 6.61 |  |  |
| 129.5 | 6.70 |  |  |
| 130 | 6.80 |  |  |
| 131 | 6.96 |  |  |
| 132 | 7.11 |  |  |
| 142 | 8.05 |  |  |
| 13 | 8.14 |  |  |
| 147 | 8.76 |  |  |
| 149 | 9.14 |  |  |
| 151 | 9.50 |  |  |
| 152 | 9.68 |  |  |

| TABLE A1.29 Load vs. Displacement data for spec. 30 $(a/w=0.42, P_{max}=12\ kg)$ | | TABLE A1.30 Displacement vs. Time data for spec. 30 $(a/w=0.42, P_{max}=12\ kg)$ | |
|---|---|---|---|
| LOAD (kg) | DISPL. (mm) | TIME (hrs) | DISPL. (mm) |
| 0 | 0 | 0 | 0 |
| 3 | 0.99 | 1 | 0.27 |
| 5 | 1.62 | 2 | 0.37 |
| 7 | 2.28 | 3 | 0.42 |
| 9 | 2.97 | 4 | 0.47 |
| 10 | 3.33 | 7 | 0.56 |
| 11 | 3.73 | 22 | 0.84 |
| 12 | 4.21 | 24.5 | 0.89 |
| | | 27 | 0.94 |
| | | 29 | 0.98 |
| | | 47 | 1.34 |
| | | 51 | 1.43 |
| | | 53 | 1.48 |
| | | 59 | 1.63 |
| | | 69.5 | 1.86 |
| | | 72 | 1.92 |
| | | 74 | 1.97 |
| | | 78 | 2.10 |
| | | 79 | 2.13 |
| | | 80 | 2.16 |
| | | 95 | 2.56 |
| | | 100 | 2.70 |
| | | 102 | 2.75 |
| | | 118 | 3.14 |
| | | 123 | 3.28 |
| | | 142 | 4.03 |
| | | 143 | 4.04 |
| | | 144.5 | 5.08 |

TABLE A1.31 *Displacement vs Time curve*
*for spec. 31 (creep spec.*
$a/w=0.46$, $P_{max}=12.5$ kg)

| TIME (hrs) | DISPL.(mm) |
|------------|------------|
| 0 | 0 |
| 1 | 1.48 |
| 1.5 | 1.56 |
| 3.5 | 1.88 |
| 7 | 2.04 |
| 13 | 2.16 |
| 16 | 2.18 |
| 18 | 2.19 |
| 20 | 2.20 |
| 26 | 2.26 |
| 31 | 2.27 |
| 40 | 2.29 |
| 64 | |
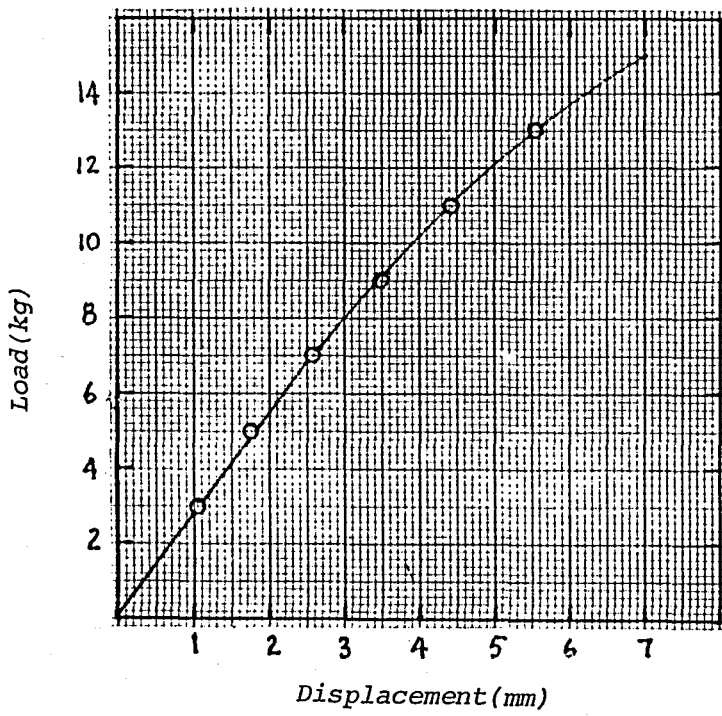
FIGURE Al.1 Load vs. Displacement curve for spec. 12
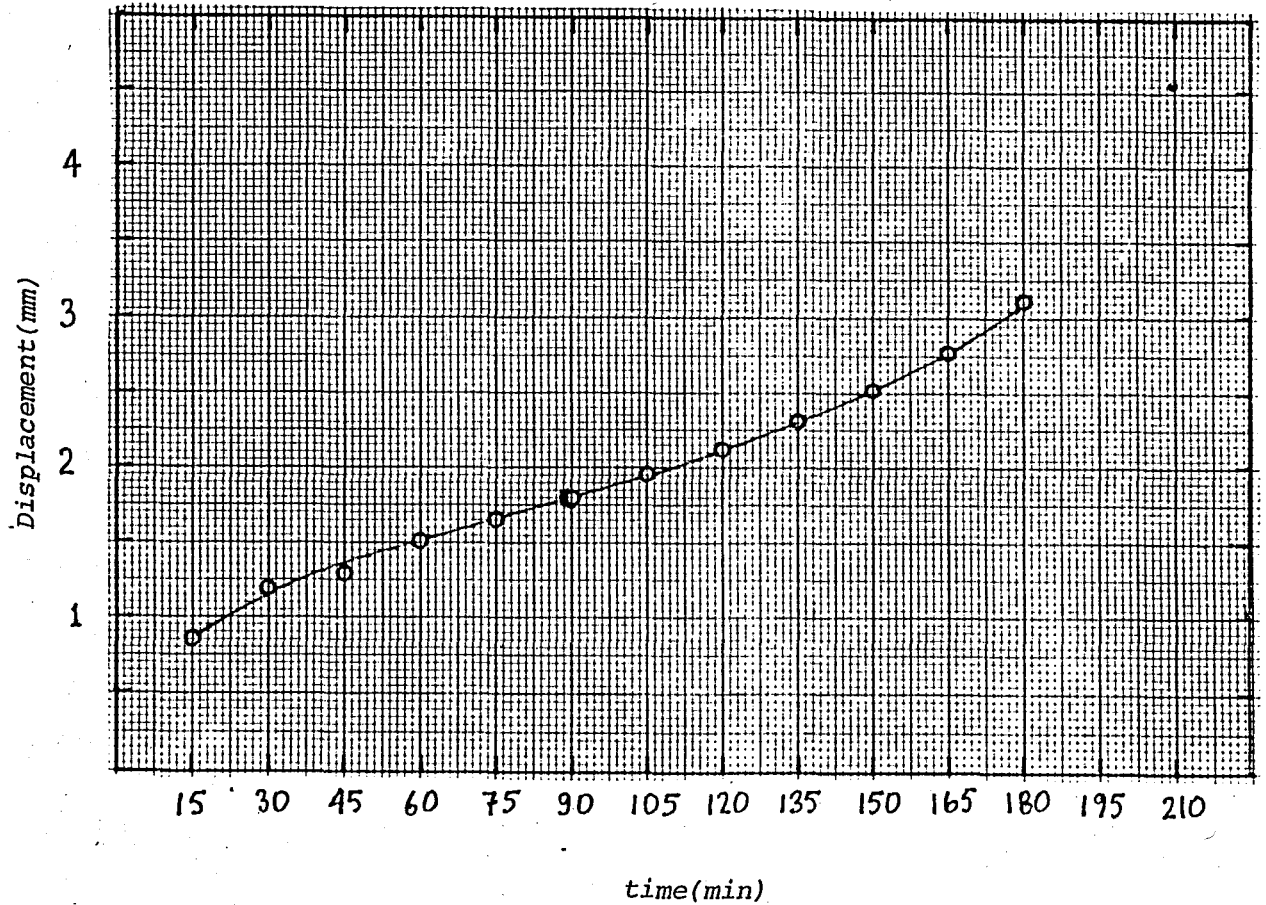


time(min)

FIGURE Al.2 Displacement vs Time curve for spec.12
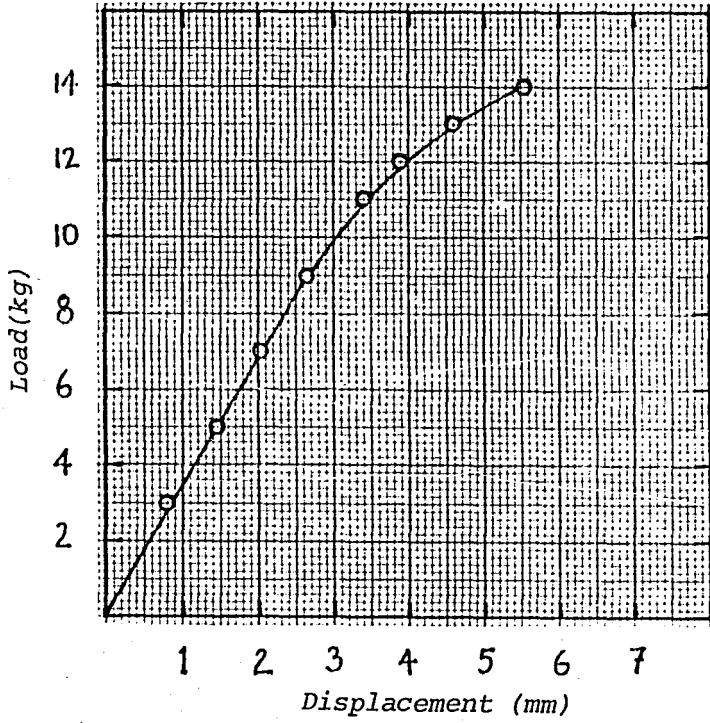
FIGURE Al.3 Load vs. Displacement curve for spec.13
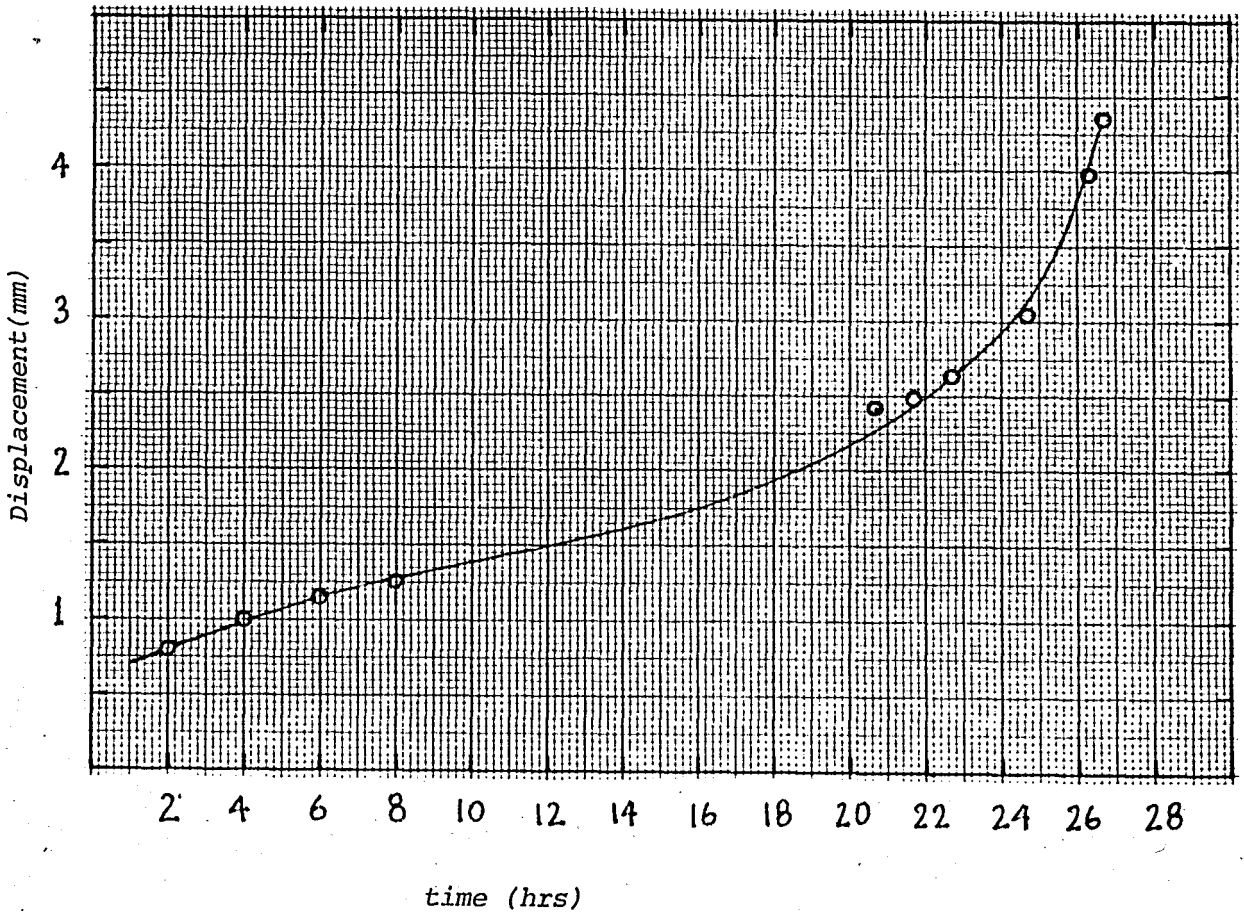


time (hrs)

FIGURE Al.4 Displacement vs. Time curve for spec.13

Displacement (mm)
FIGURE Al.5 Load vs. Displacement curve for spec.14
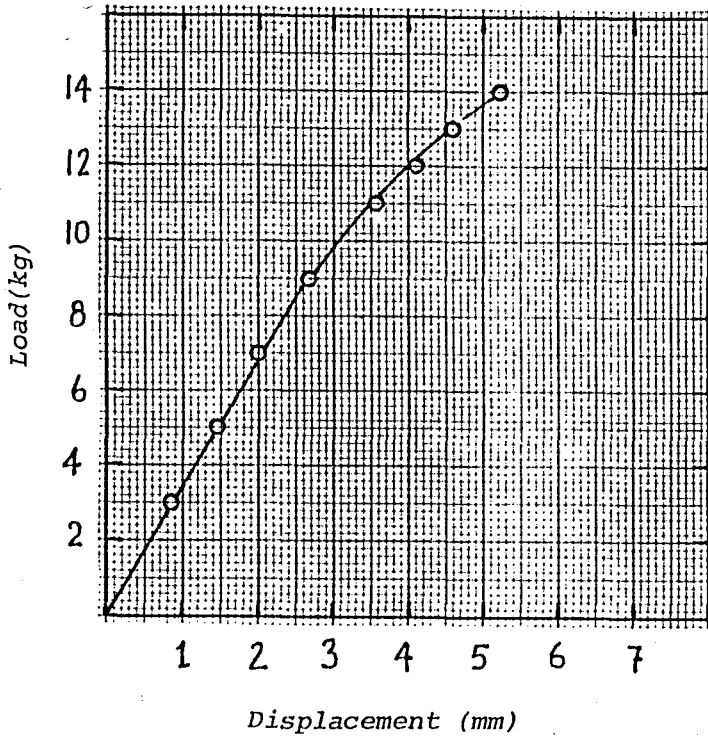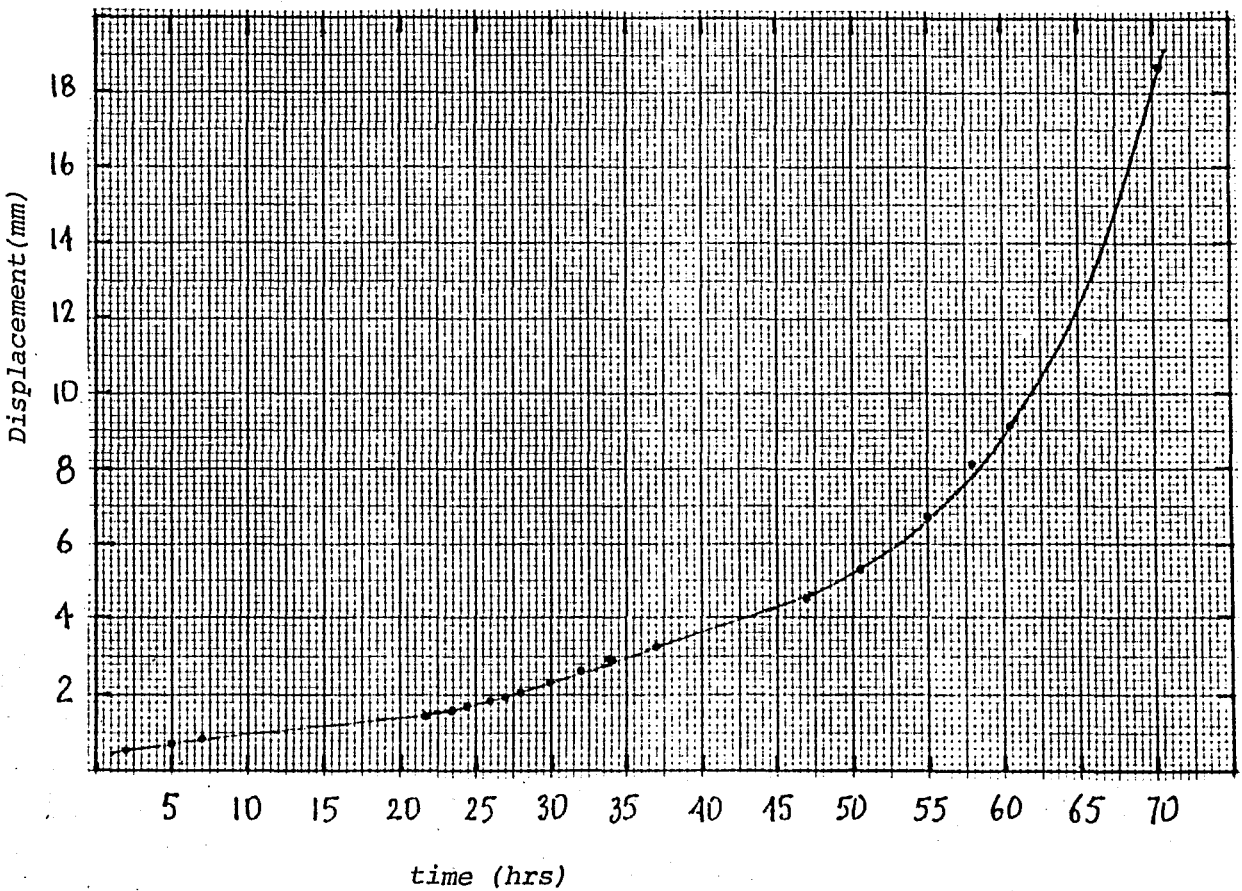


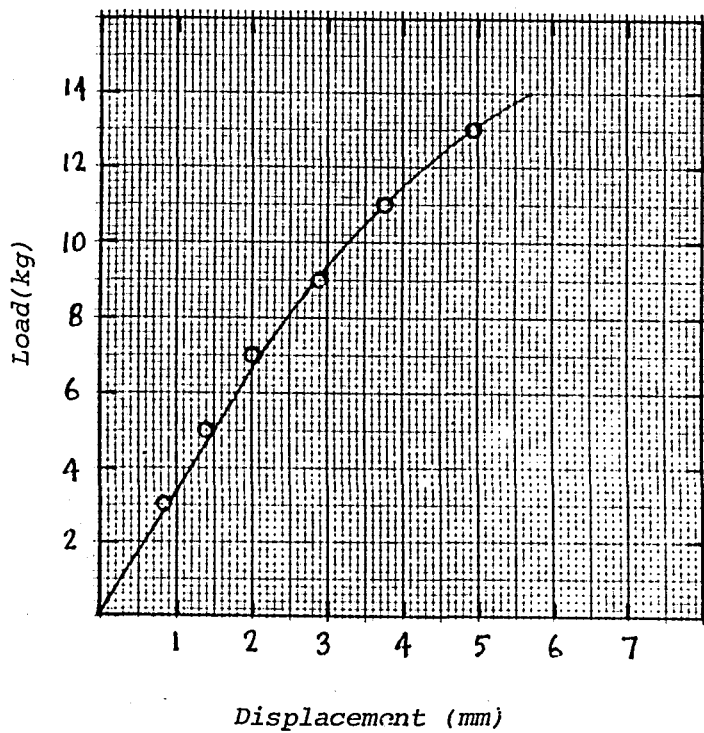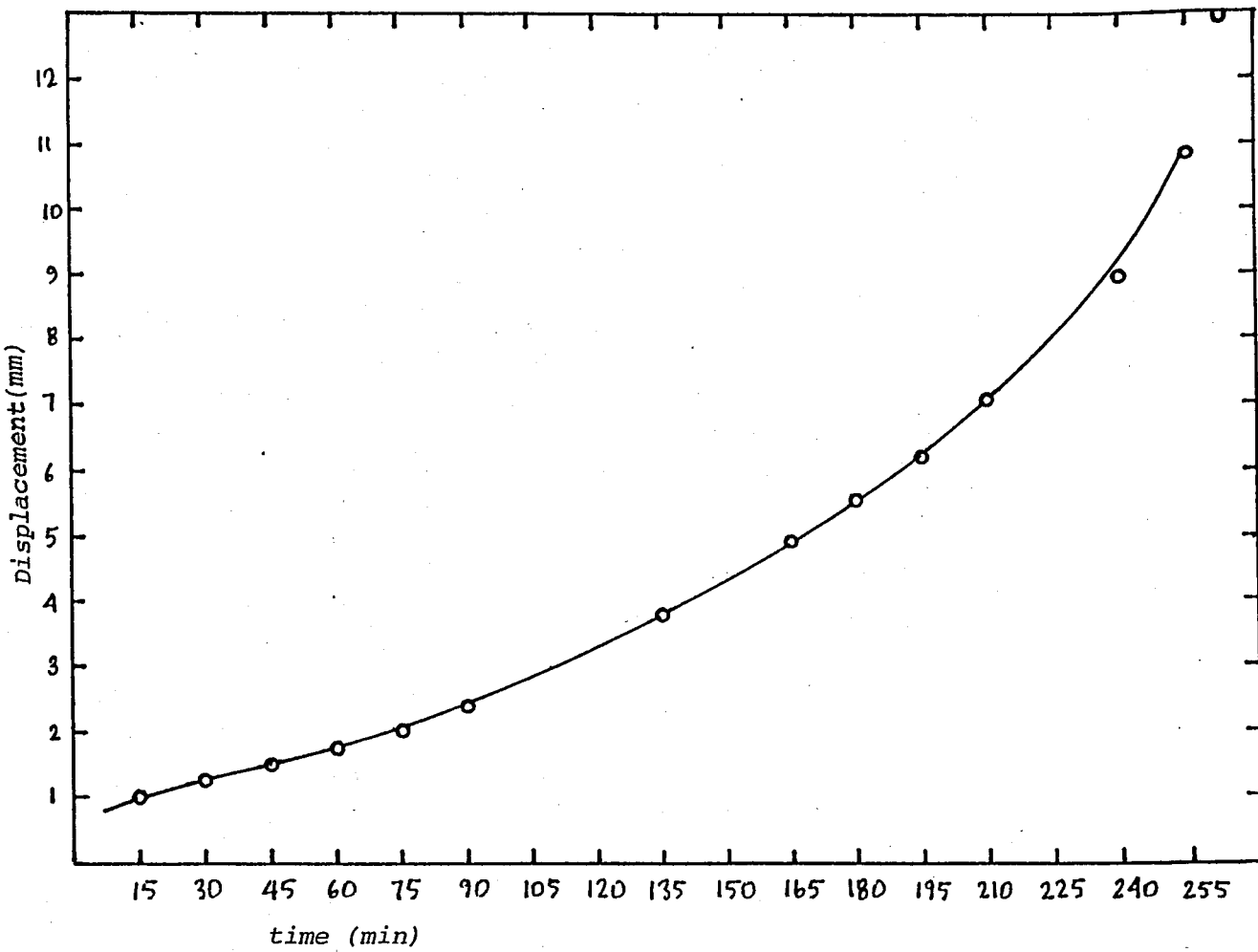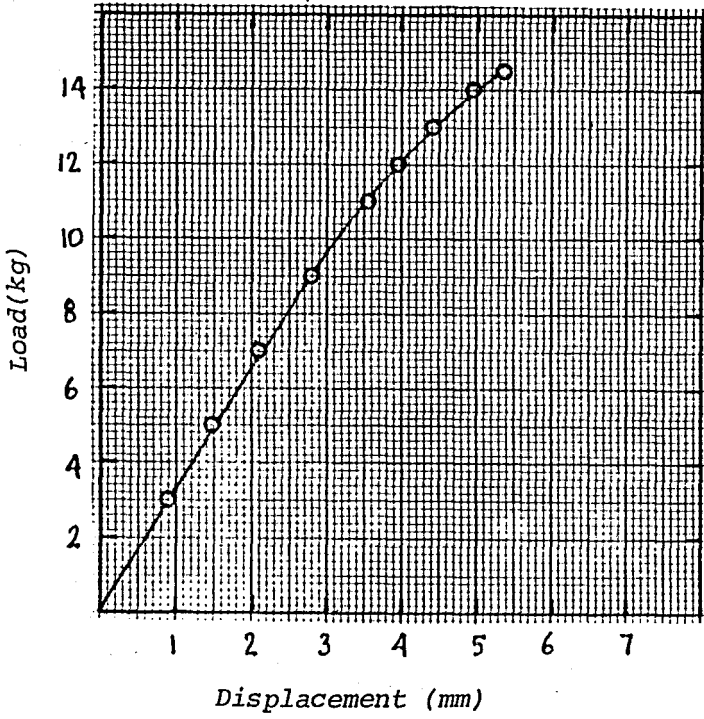time (hrs)
FIGURE Al.6 Displacement vs. Time curve for spec.14
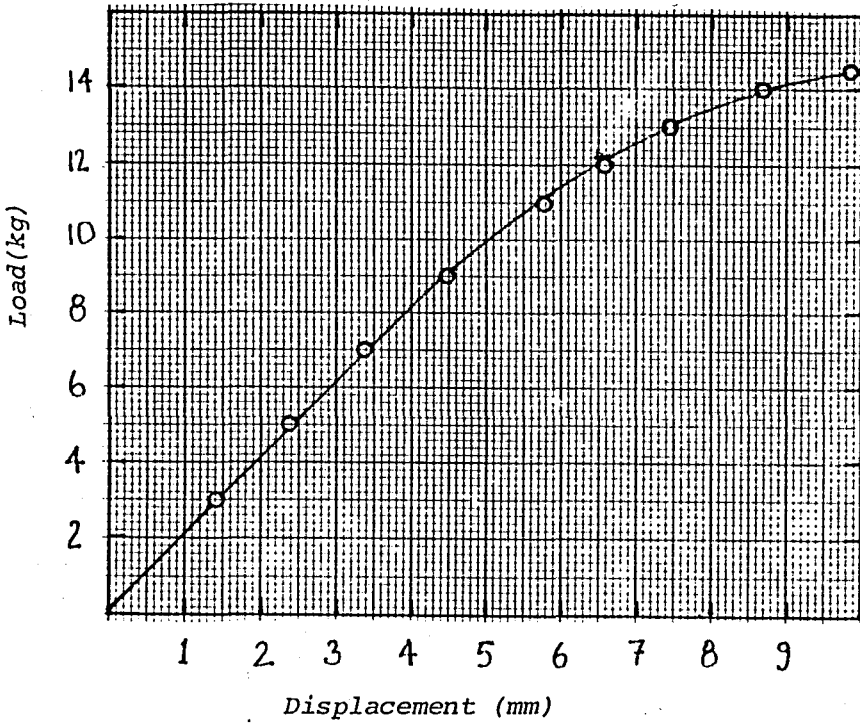
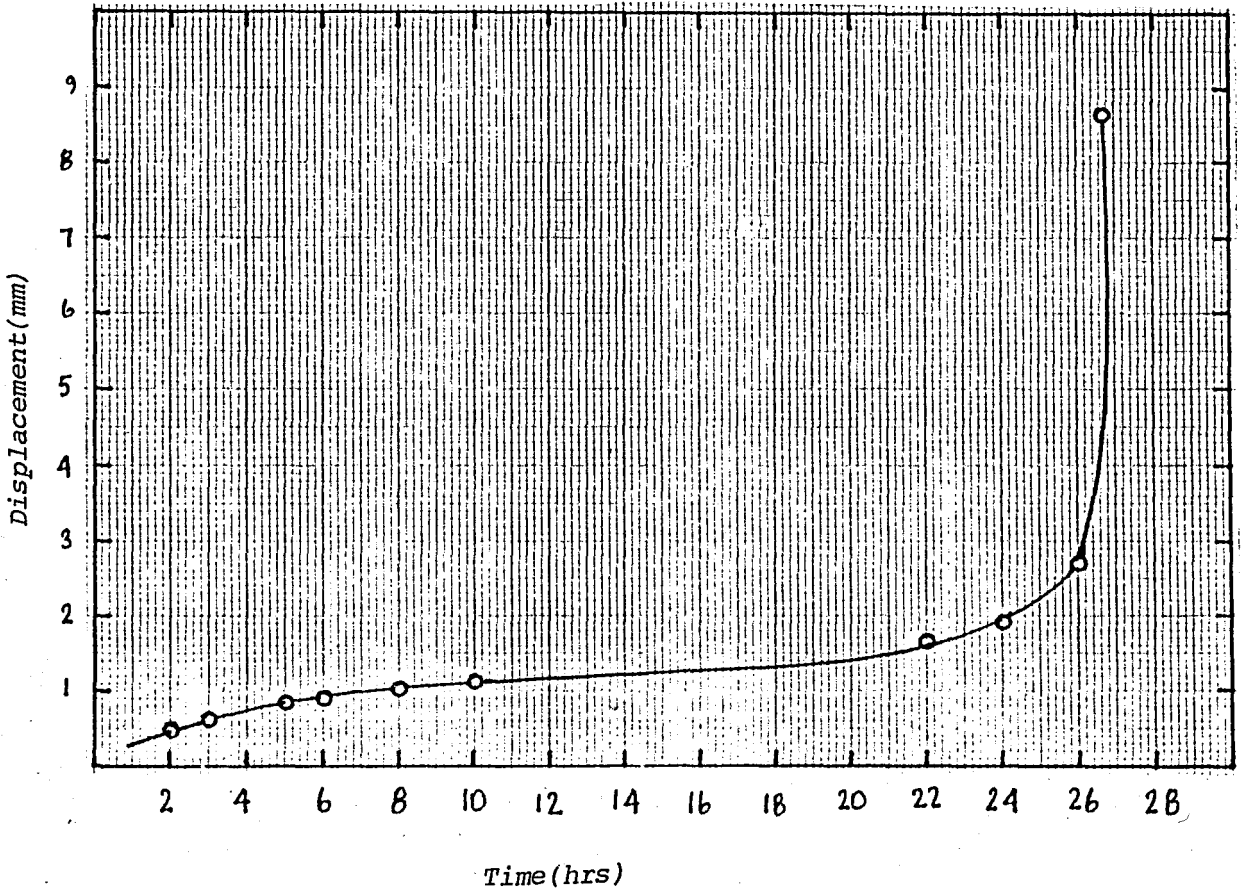FIGURE A1.7 Load vs. Displacement curve for spec.15



time(min)
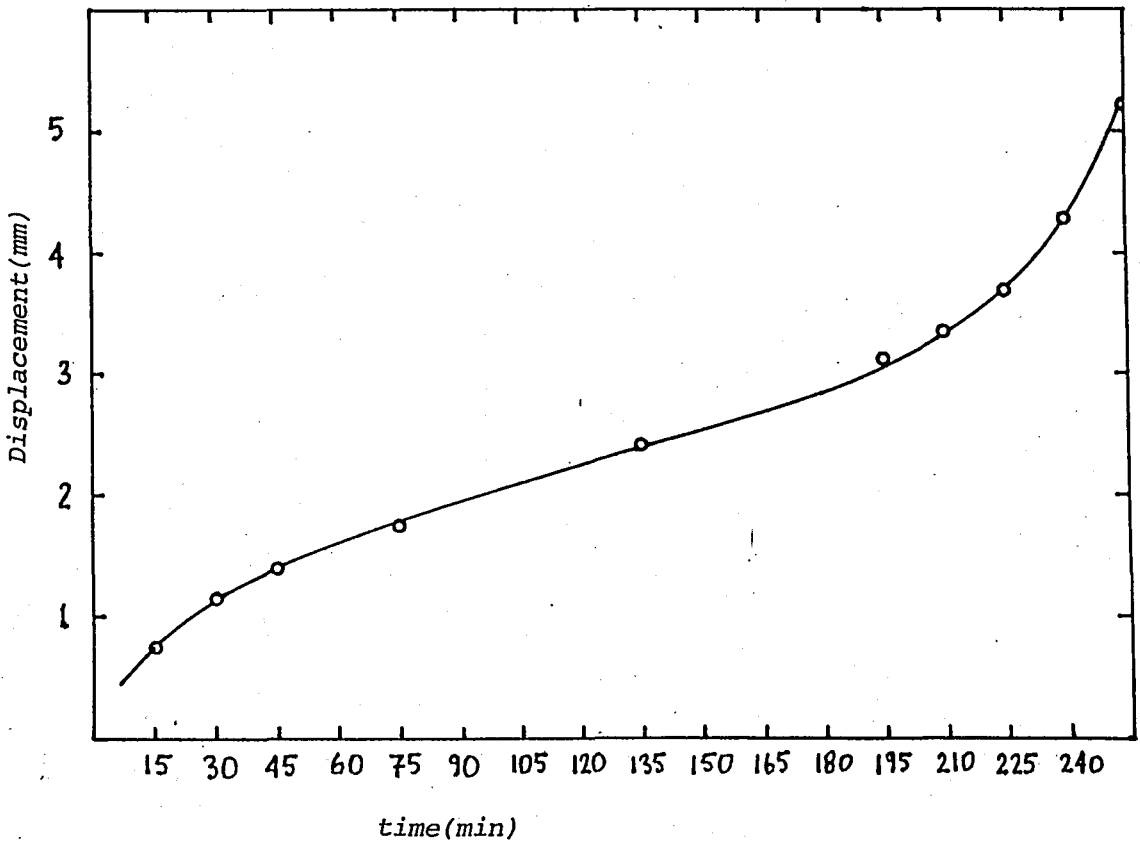
FIGURE A1.8 Displacement vs. Time curve for spec.15
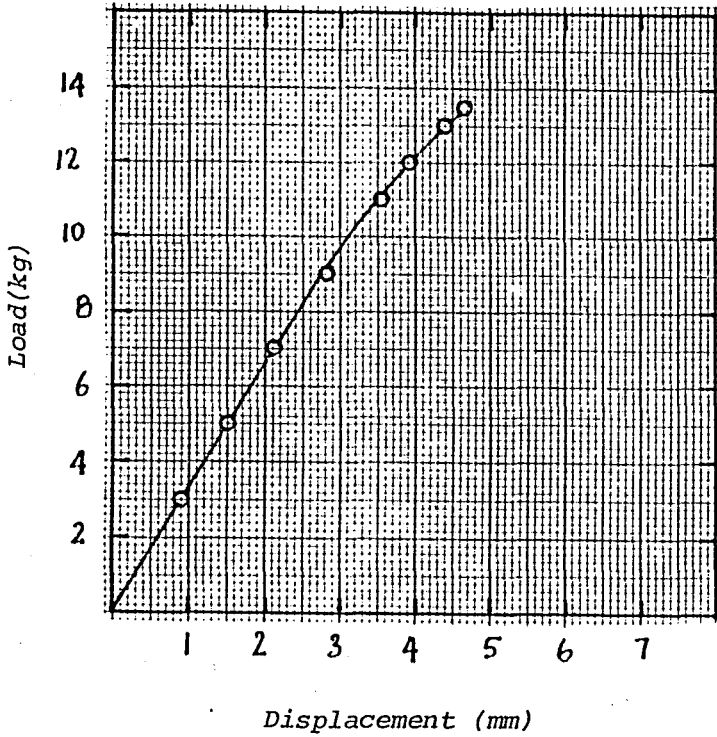
Displacement (mm)
FIGURE A1.9   Load vs. Displacement curve for spec.16
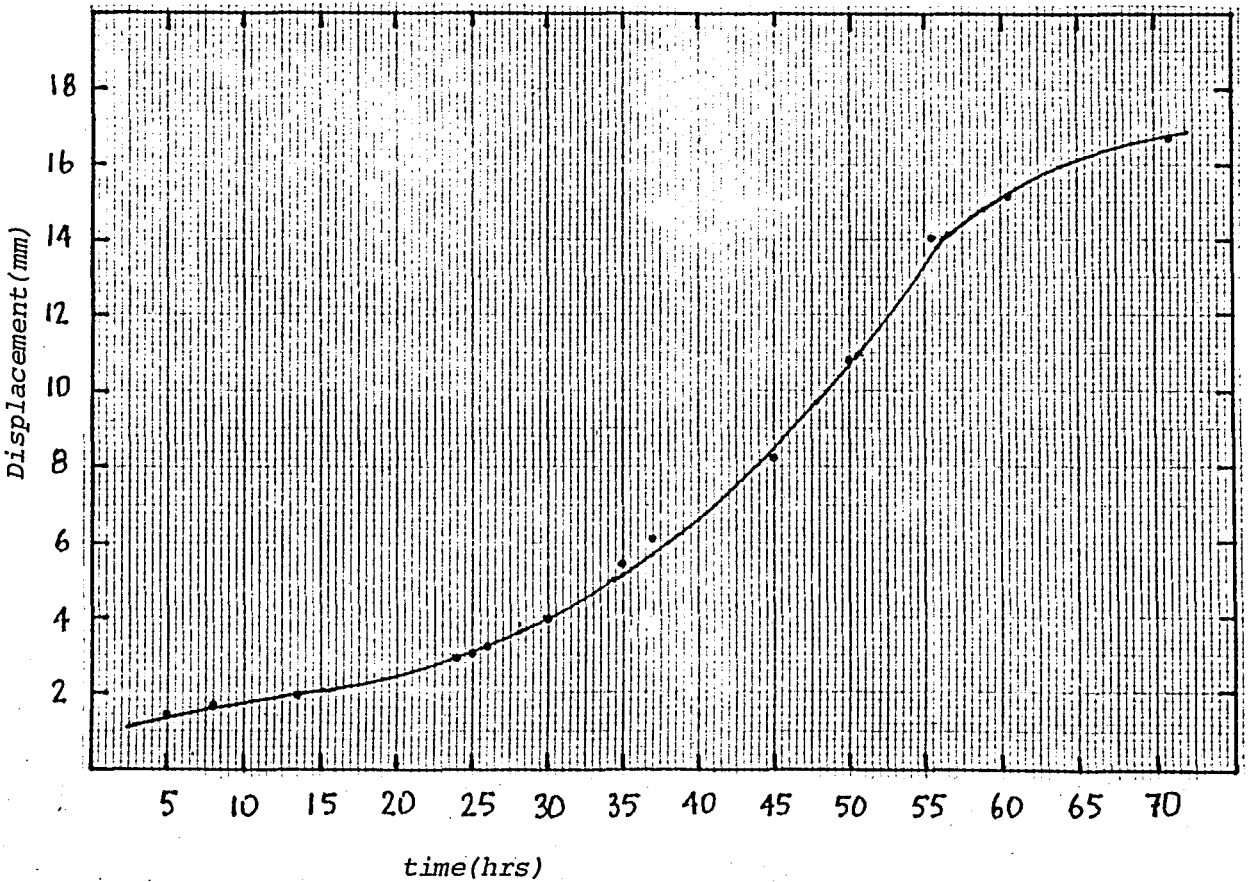


time(hrs)
FIGURE A1.10Displacement vs. time curve for spec.16
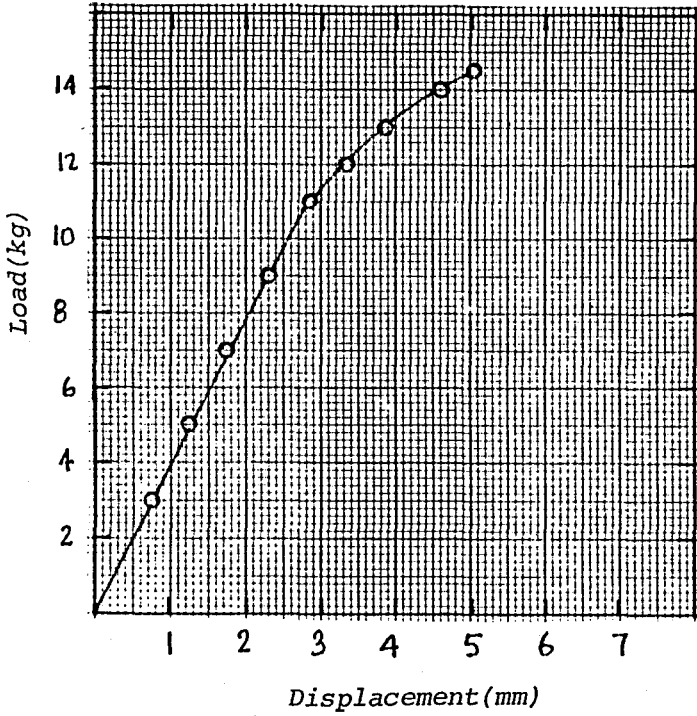
FIGURE A1.11 Load vs. Displacement curve for spec.19



time(hrs)
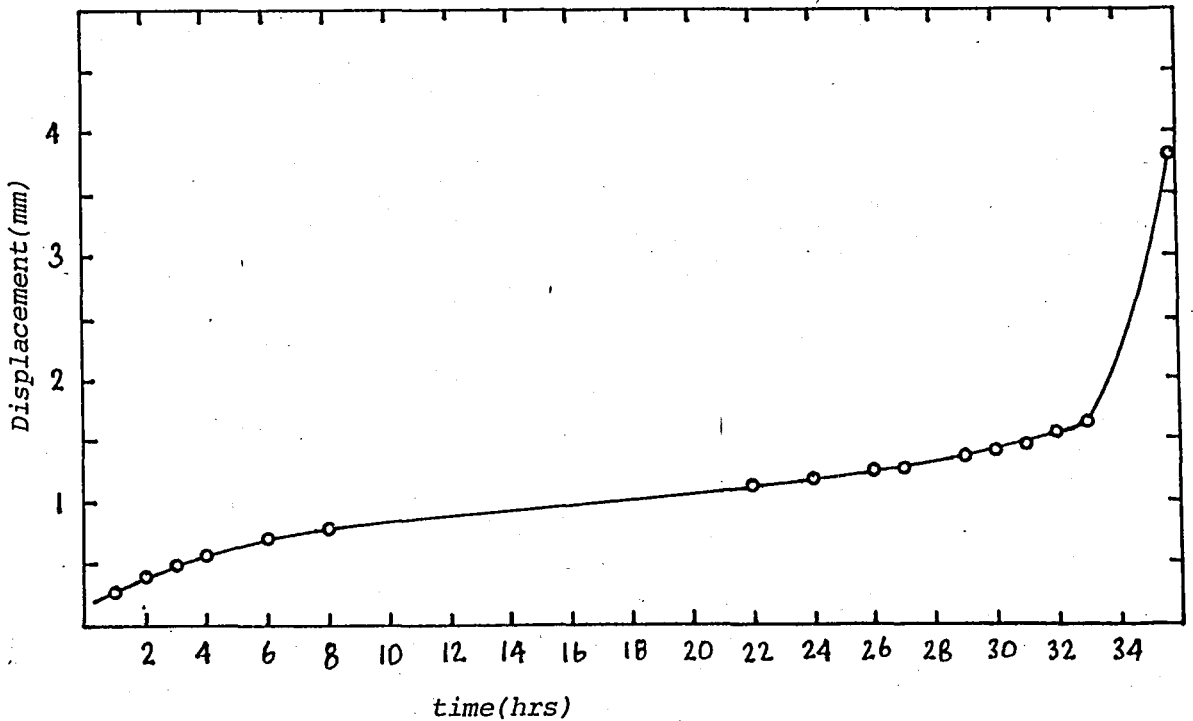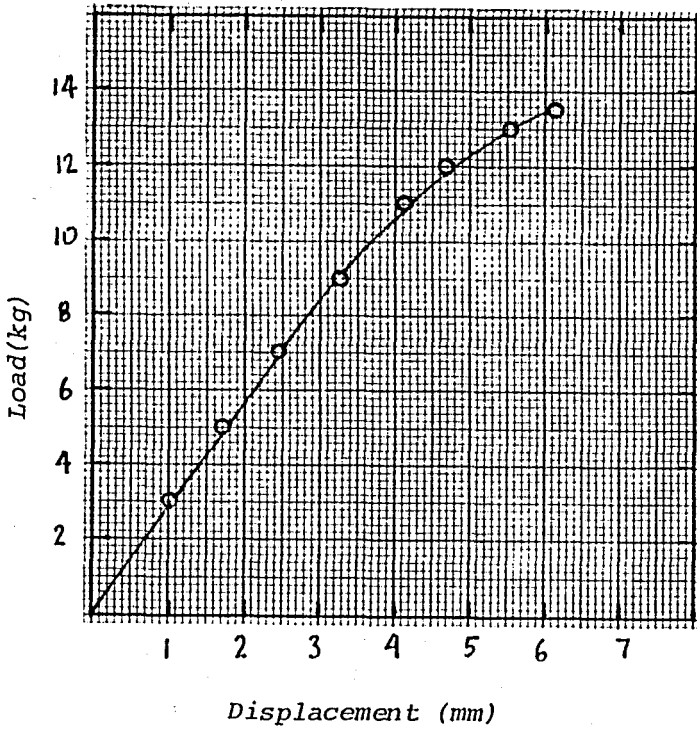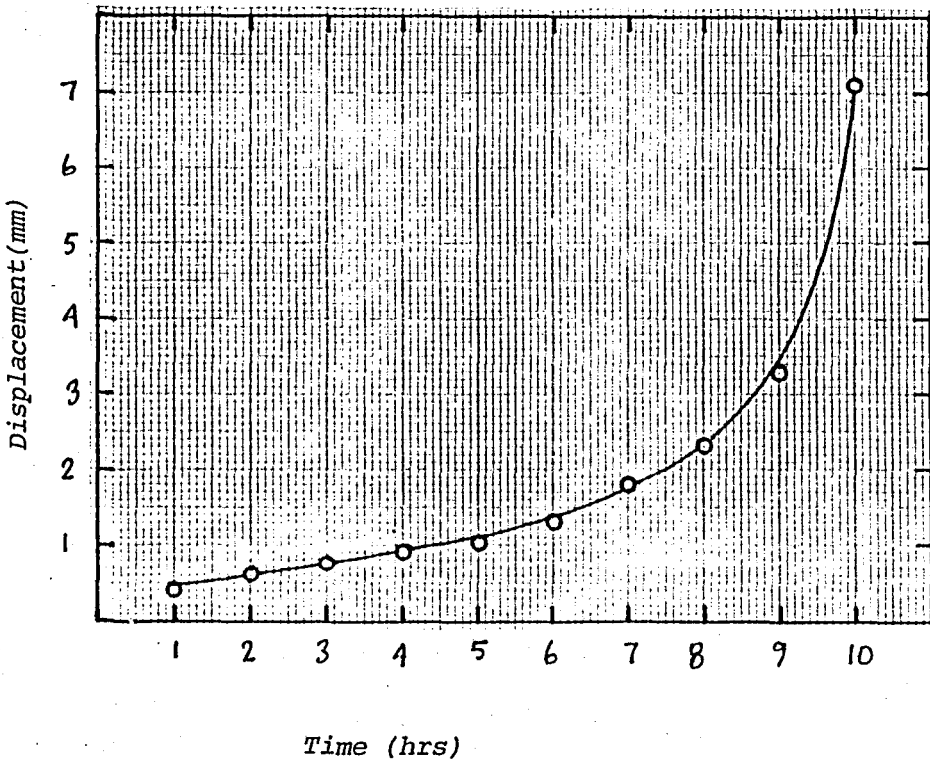
FIGURE A1.12 Displacement vs. Time curve for spec.19
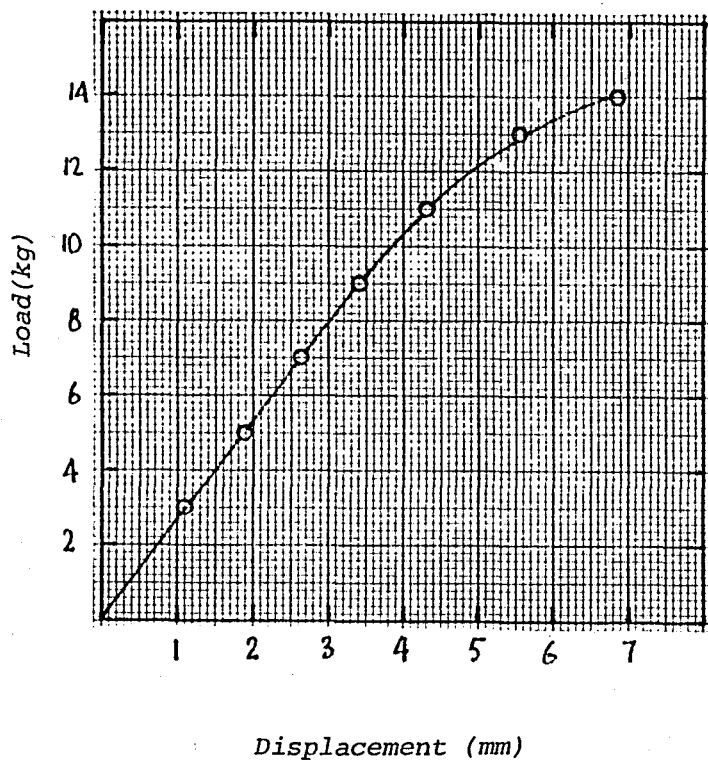
Displacement (mm)
FIGURE A1.13 Load vs. Displacement curve for spec.20
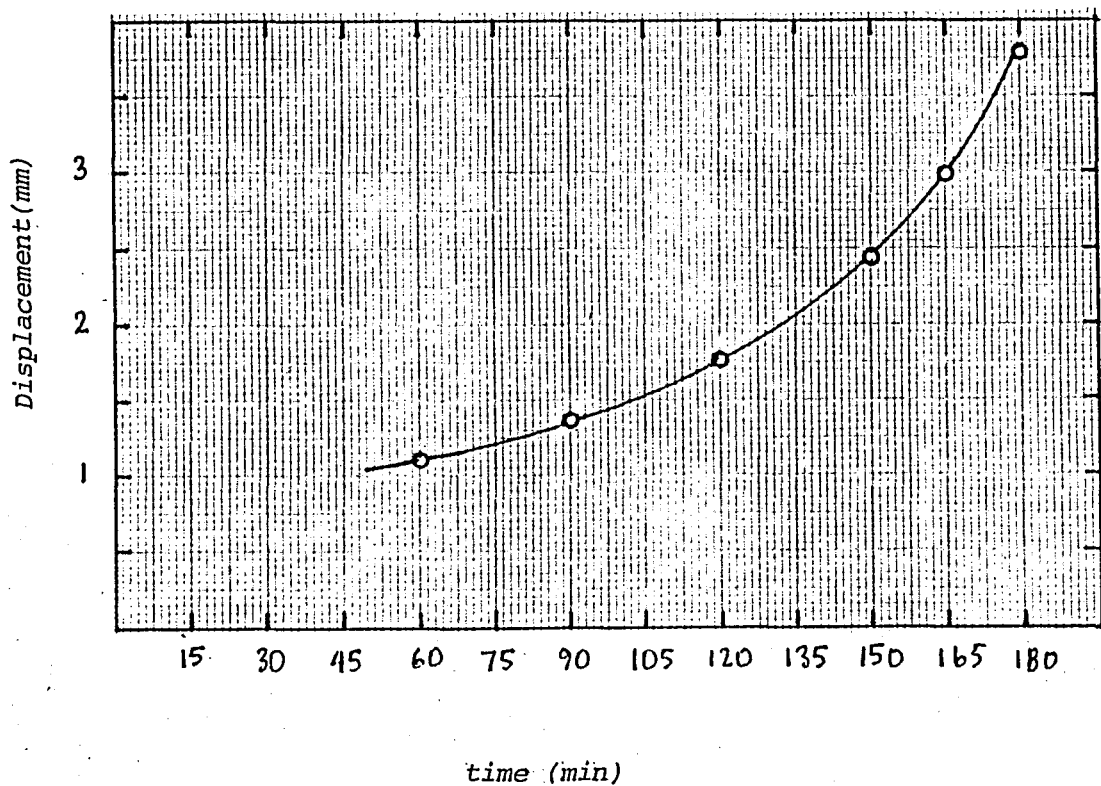


time (min)
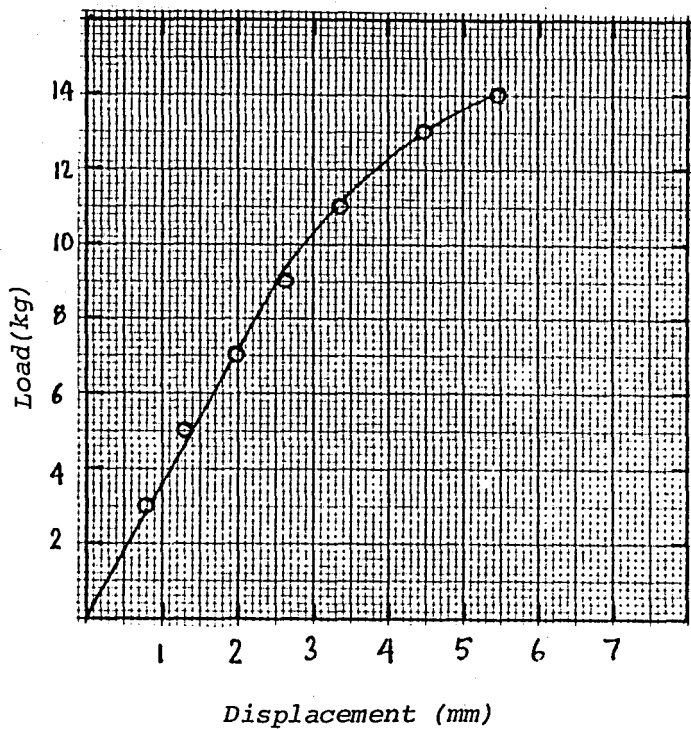FIGURE A1.14 Displacement vs. Time curve for spec.20

*Displacement (mm)*
*FIGURE Al.15 Load vs. Displacement curve for spec.22*

FIGURE Al.16 Displacement vs. time curve for spec.22
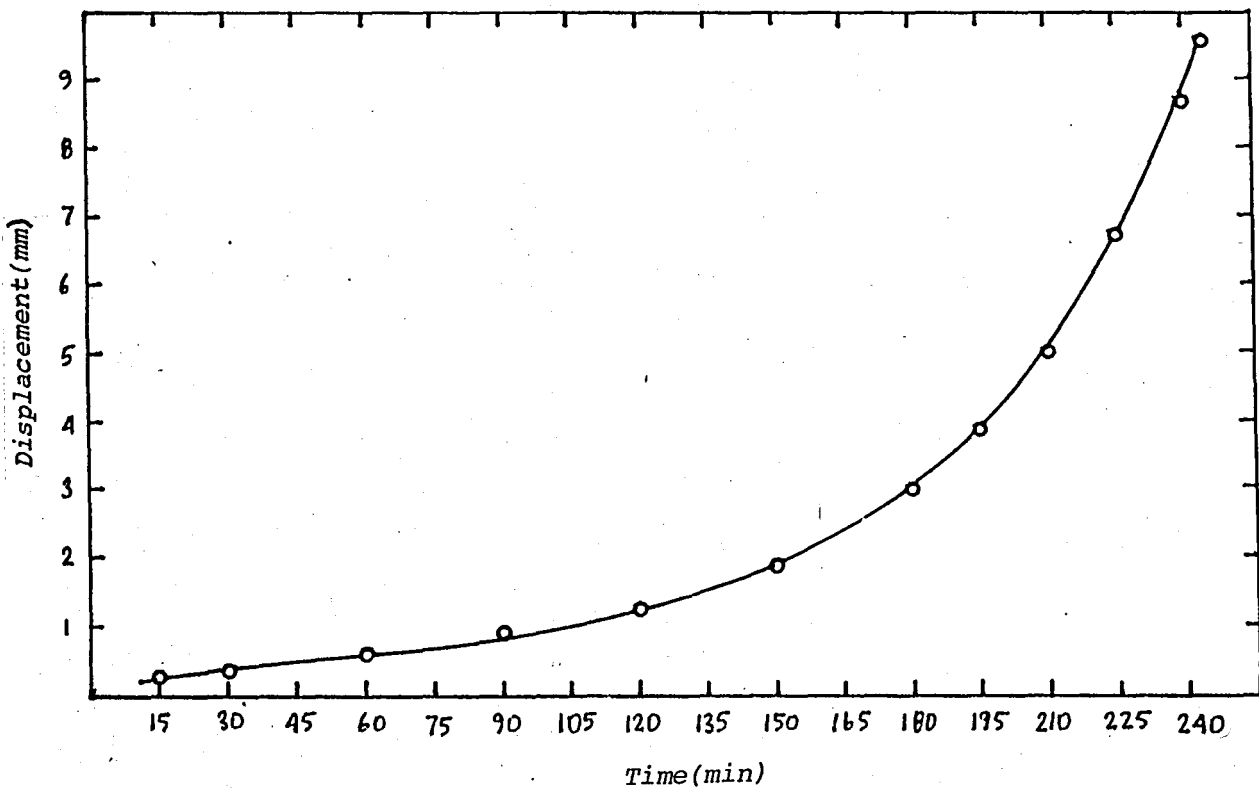
FIGURE A1.17 Load vs. Displacement curve for spec. 23
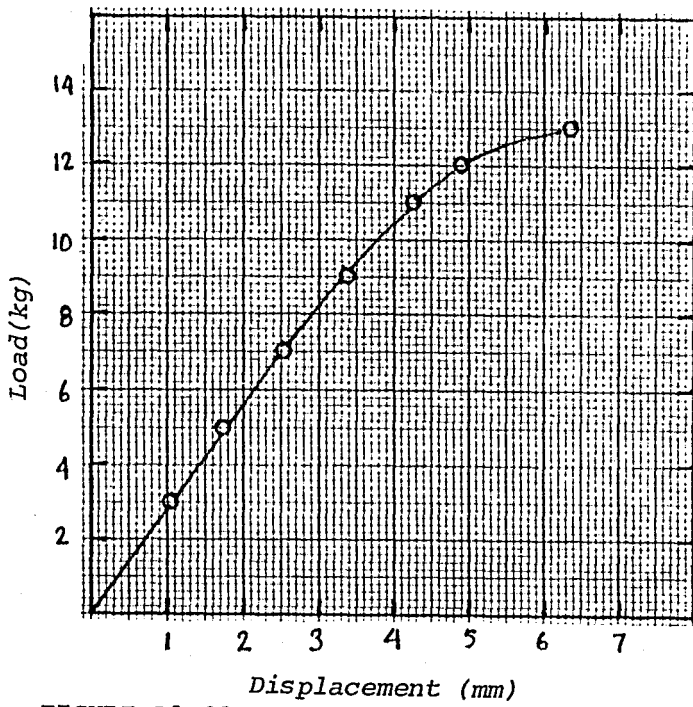


FIGURE A1.18 Displacement vs.Time curve for specimen 23

Displacement (mm)
FIGURE A1.19 Load vs. Displacement curve for spec.24



Time (hrs)
FIGURE A1.20 Displacement vs.Time curve for spec. 24

Displacement (mm)

FIGURE A1.21 Load vs.Displacement curve for spec.25



Time(min)

FIGURE A1.22 Displacement vs. Time curve for spec.25

FIGURE A1.23 Load vs. Displacement curve for spec.26
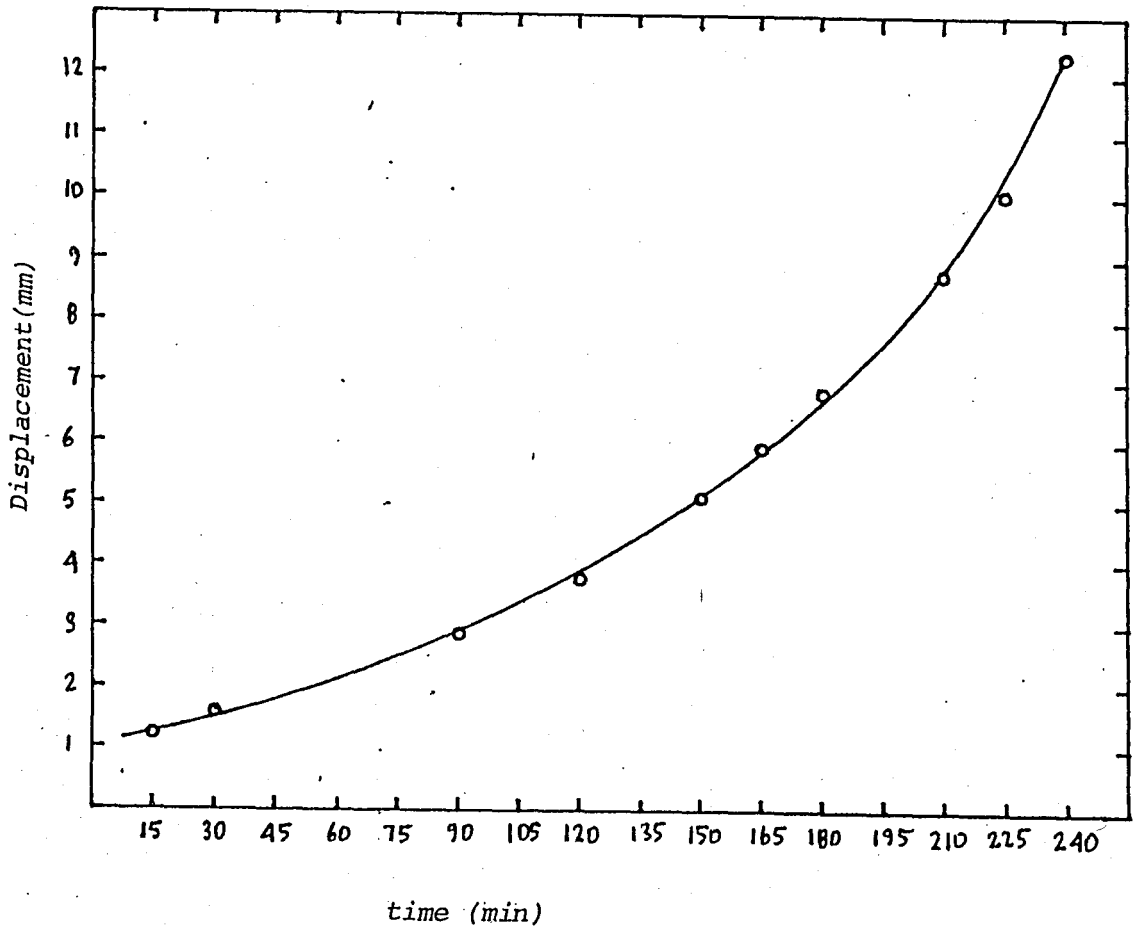


time (min)

FIGURE A1.24 Displecement vs. time curve for spec.26

FIGURE A1.25 Load vs. Displacement curve for spec.27
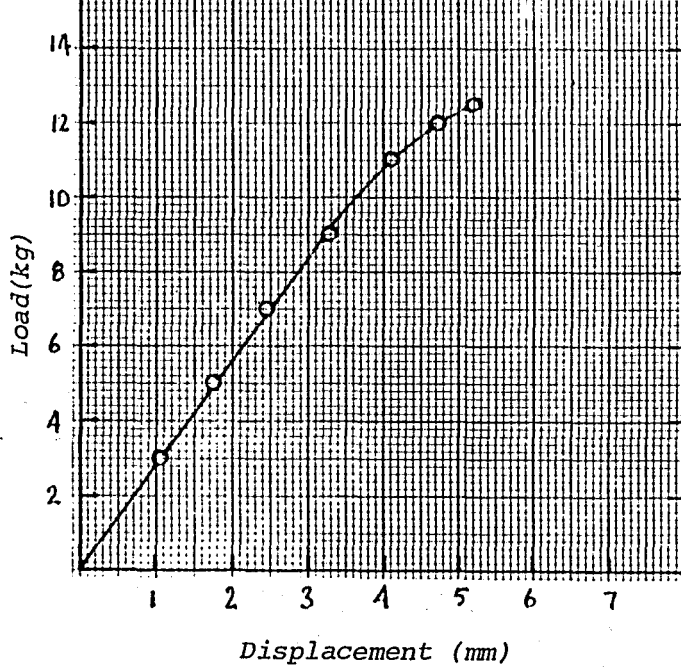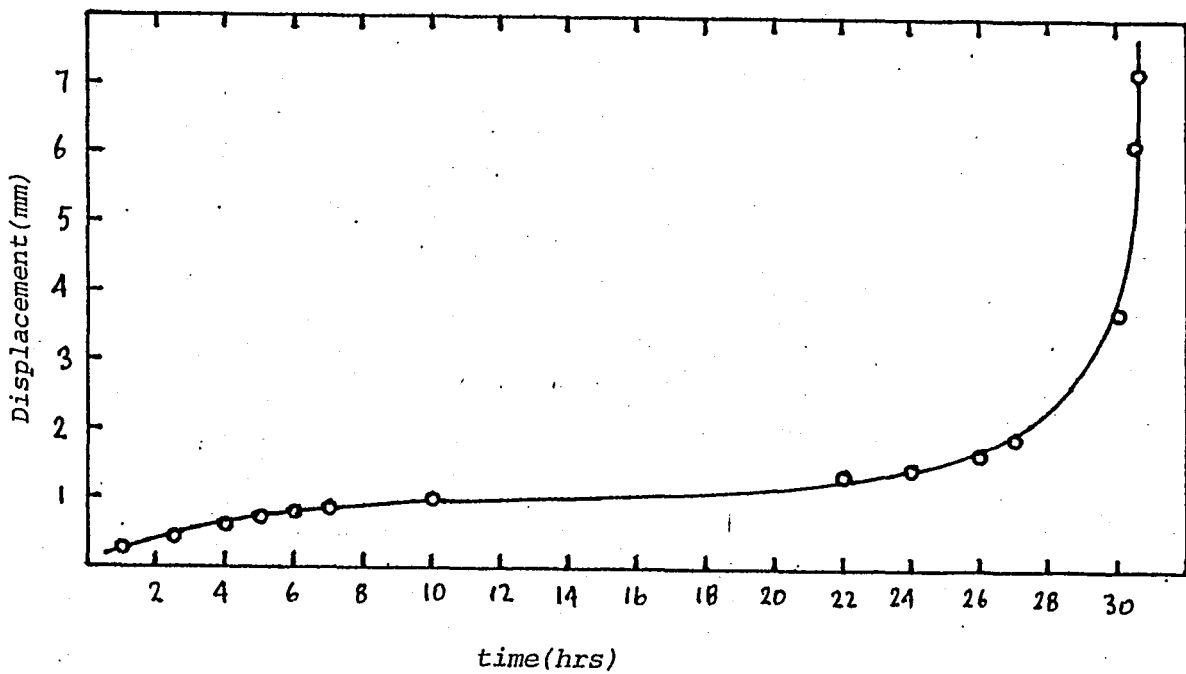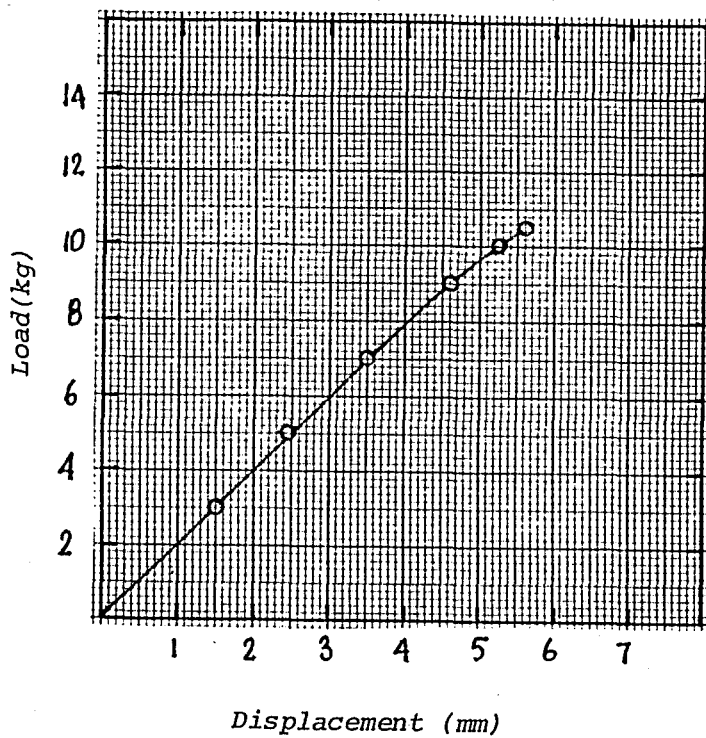


FIGURE A1.26 Displacement vs. Time curve for spec. 27

Displacement (mm)

FIGURE A1.27 Load vs. Displacement curve for spec.28



Time(hrs)

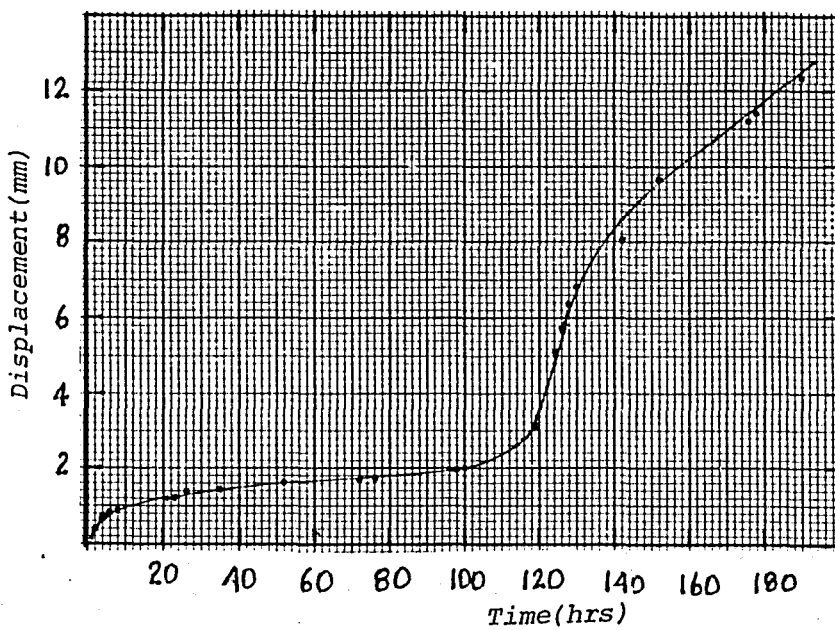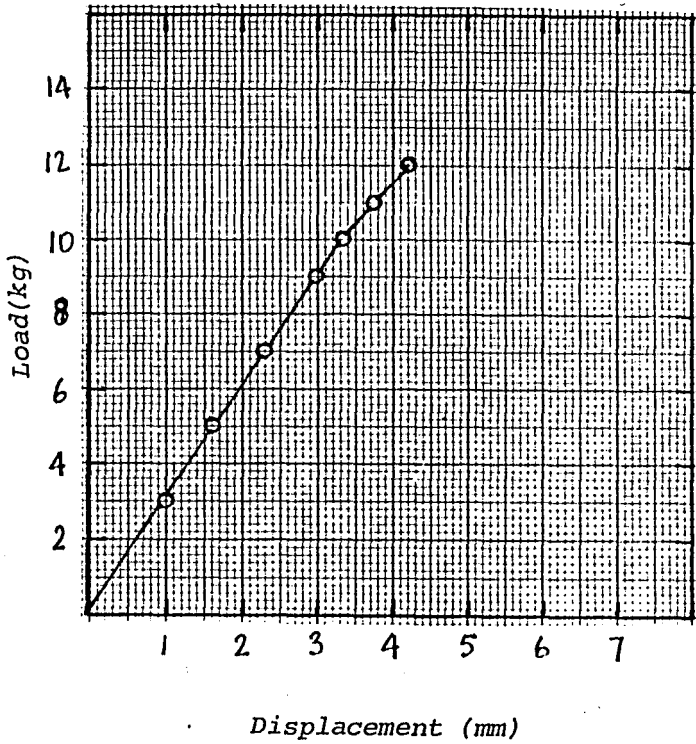FIGURE A1.28 Displacement vs. Time curve for spec.28

Displacement (mm)

FIGURE A1.29 Load vs. Displacement curve for spec.30
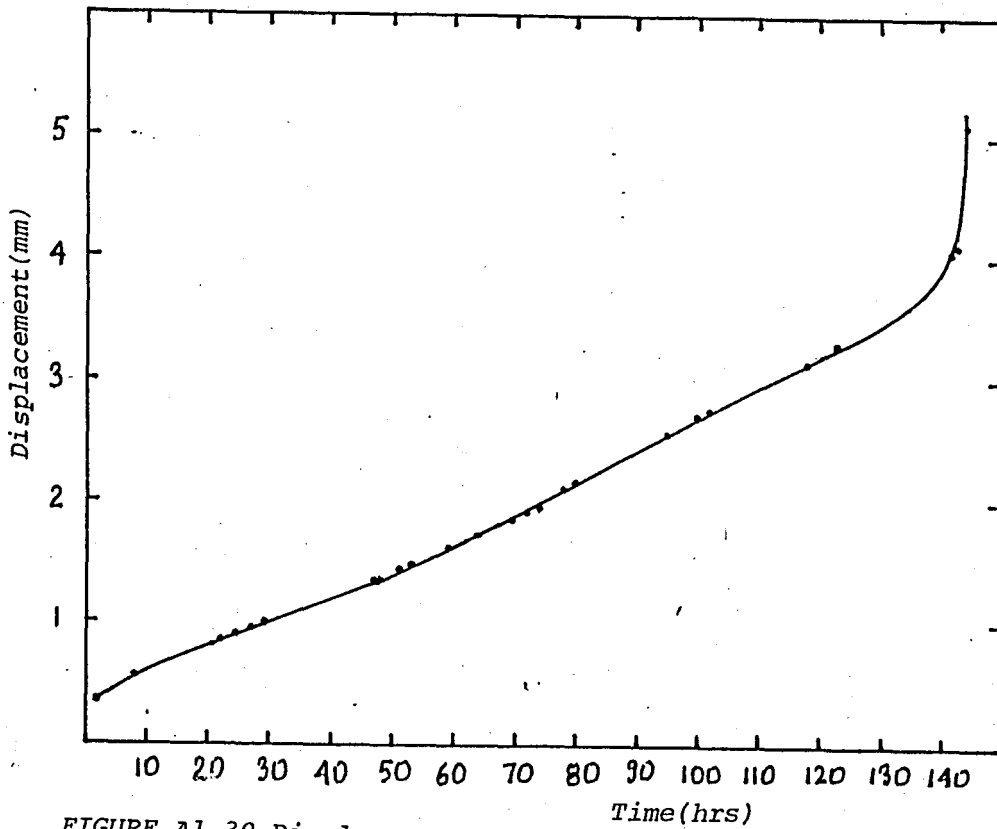


Time(hrs)

FIGURE A1.30 Displacement vs.Time curve for spec.30

# APPENDIX 2

## DATA AND GRAPHS OBTAINED
## TO RE-EVALUATE THE J-INTEGRAL
## VALUES

TABLE A2.1 *Points of the Compliance*
          *calibration curve on*
          *Figure 5.8*

| CEB | a/w |
|-----|-----|
| $5.97 \times 10^6$ | 0.29 |
| $6.26 \times 10^6$ | 0.36 |
| $6.31 \times 10^6$ | 0.38 |
| $6.52 \times 10^6$ | 0.40 |
| $6.61 \times 10^6$ | 0.43 |
| $7.13 \times 10^6$ | 0.45 |
| $7.70 \times 10^6$ | 0.50 |

TABLE A2.2 Load vs Displacement data obtained to determine $\Delta_{max}$ for each $P_{max}$ value on Table 5.2

a/W = 0.38

| LOAD (kg) | DISPL.(mm) |
|---|---|
| 0 | 0 |
| 3 | 1.13 |
| 5 | 1.88 |
| 7 | 2.63 |
| 9 | 3.38 |
| 11 | 4.18 |
| 12 | 4.68 |
| 12.5 | 4.93 |
| 13 | 5.18 |
| 13.5 | 5.43 |
| 14 | 5.73 |
| 14.5 | 6.08 |
| 15 | 6.53 |

TABLE A2.3 Load vs.Displacement data obtained to determine $\Delta_{max}$ for each $P_{max}$ value on Table 5.2

a/W = 0.40

| LOAD (kg) | DISPL.(mm) |
|---|---|
| 0 | 0 |
| 3 | 1.15 |
| 5 | 1.91 |
| 7 | 2.61 |
| 9 | 3.36 |
| 11 | 4.16 |
| 12 | 4.61 |
| 12.5 | 4.86 |
| 13 | 5.11 |
| 13.5 | 5.51 |
| 14 | 5.81 |
| 14.5 | 6.36 |
| 15 | 6.86 |

TABLE A2.4 Load vs. Displacement data obtained to determine the $\Delta_{max}$ values for each $P_{max}$ value on table 5.2

$a/W = 0.43$

| LOAD (kg) | DISPL. (mm) |
|-----------|-------------|
| 0 | 0 |
| 3 | 1.05 |
| 5 | 1.75 |
| 7 | 2.43 |
| 9 | 3.21 |
| 11 | 4.08 |
| 12 | 4.66 |
| 12.5 | 5.01 |
| 13 | 5.41 |
| 13.5 | 5.96 |
| 14 | 7.16 |
| 14.5 | 8.56 |

TABLE A2.5 Load vs. Displacement Data obtained to determine the $\Delta_{max}$ values for each $P_{max}$ value on Table 5.2

$a/W = 0.45$

| LOAD (kg) | DISPL. (mm) |
|-----------|-------------|
| 0 | 0 |
| 3 | 1.20 |
| 5 | 2.03 |
| 7 | 2.78 |
| 9 | 3.58 |
| 11 | 4.78 |
| 12 | 5.78 |
| 12.5 | 6.78 |

FIGURE A2.1 Load vs. Displacement curve established to determine $\Delta_{max}$ values at for each $P_{max}$ value Table 5.2
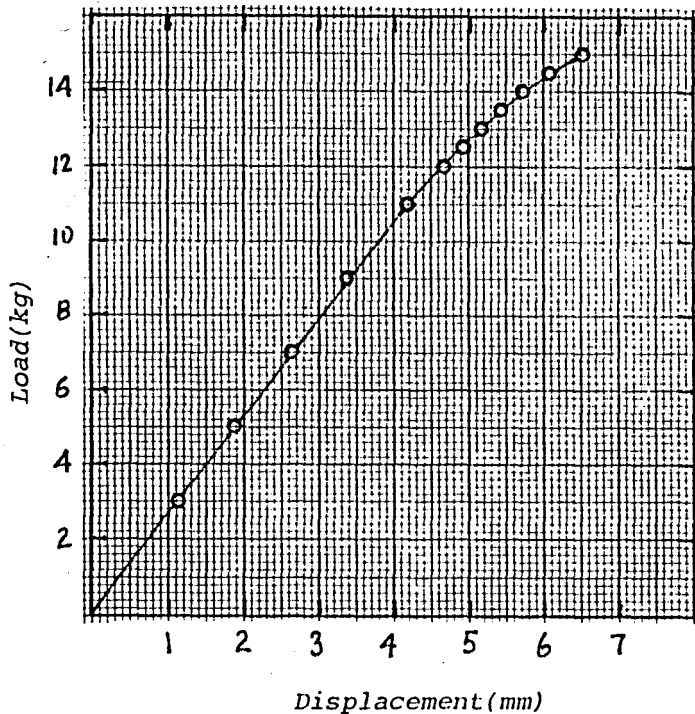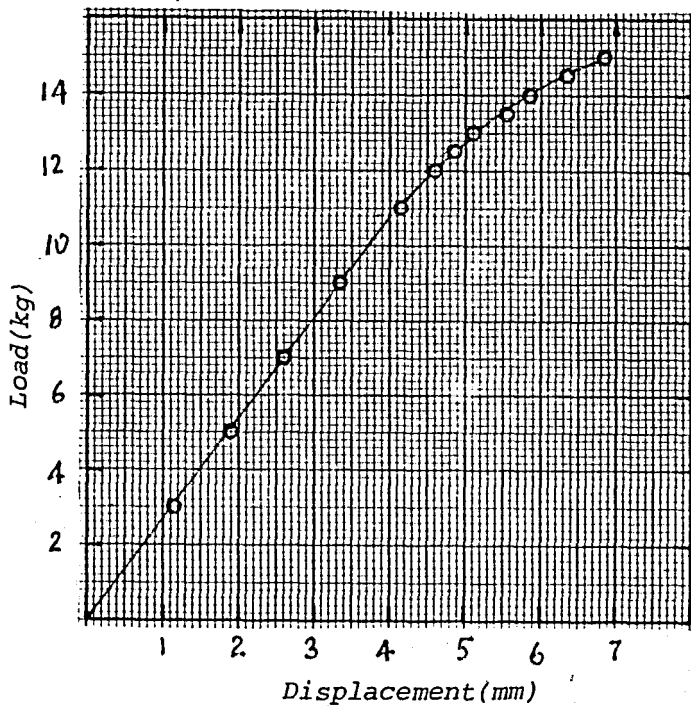


FIGURE A2.2 Load vs. Displacement curve established to determine $\Delta_{max}$ values for each $P_{max}$ value on Table 5.2
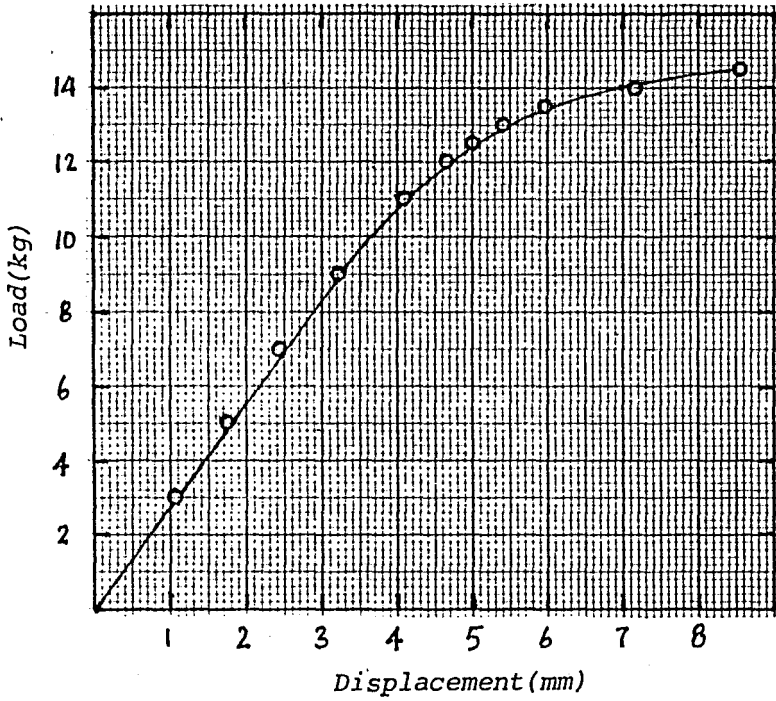a/W = 0.40

FIGURE A2.3 *Load vs. Displacement curve established
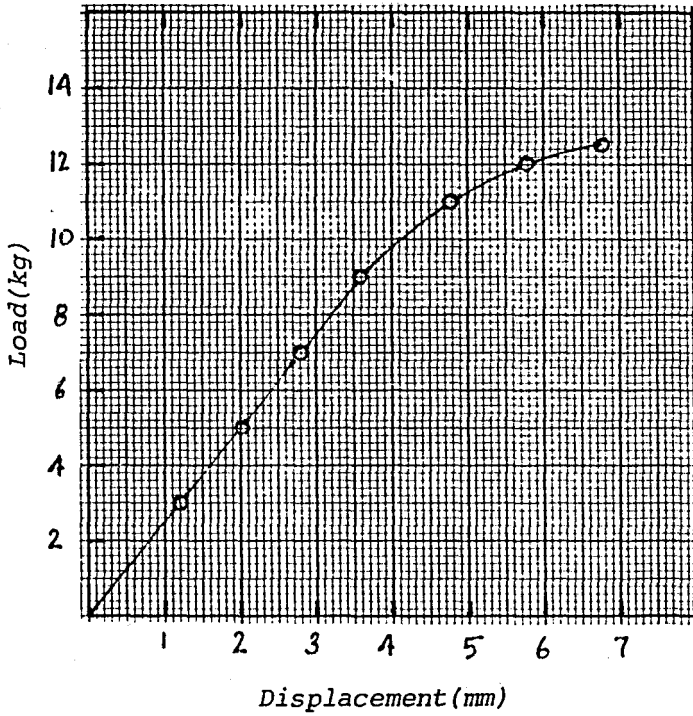to determine* $\Delta_{max}$ *values for each* $P_{max}$
*value on Table 5.2*

$a/W = 0.43$



FIGURE A2.4 *Load vs. Displacement curve established
to determine the* $\Delta_{max}$ *values for each*

$P_{max}$ *vaule on Table 5.2*

$a/W = 0.45$

TABLE A2.6 $\Delta_{max}$ as a variation of a/W and $P_{max}$ (see Fig. 5.9)

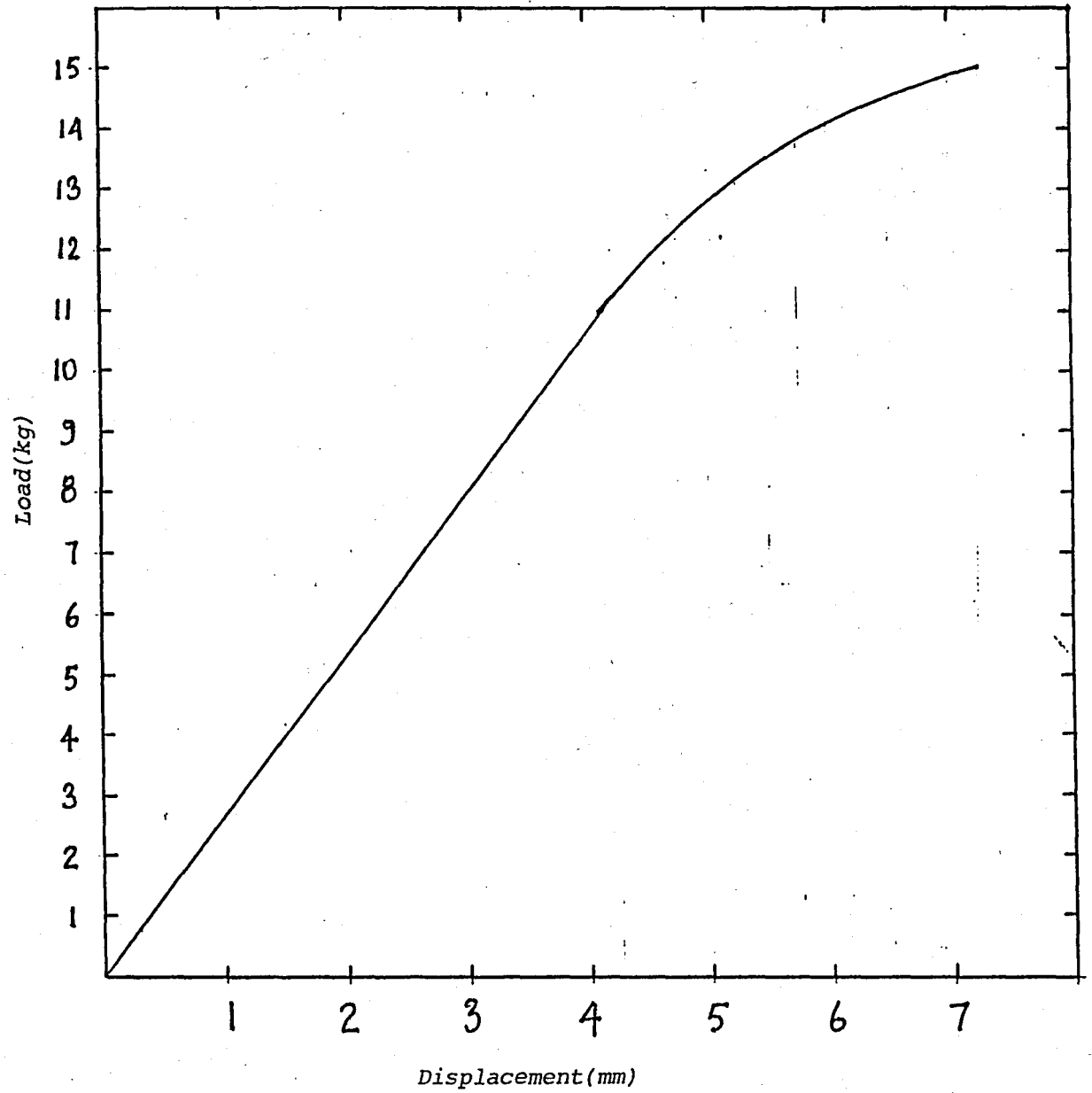| P(kg) | a/W | $\Delta_{max}$ (mm) |
|---|---|---|
| | 0.38 | 3.95 |
| | 0.40 | 3.05 |
| 10.5 | 0.43 | 4.05 |
| | 0.45 | 4.40 |
| | 0.38 | 4.90 |
| | 0.40 | 4.90 |
| 12.5 | 0.43 | 5.20 |
| | 0.45 | 6.80 |
| | 0.38 | 5.10 |
| | 0.40 | 5.10 |
| 13 | 0.43 | 5.60 |
| | 0.45 | 10.30 |
| | 0.38 | 5.40 |
| 13.5 | 0.40 | 5.45 |
| | 0.43 | 6.10 |
| | 0.38 | 5.75 |
| 14 | 0.40 | 5.80 |
| | 0.43 | 7.00 |
| | 0.38 | 6.70 |
| 14.5 | 0.40 | 6.25 |
| | 0.43 | 8.70 |
| 15 | 0.38 | 6.50 |
| | 0.40 | 6.80 |

FIGURE A2.5 Re-Plotted Load vs. Displacement curve for spec.12

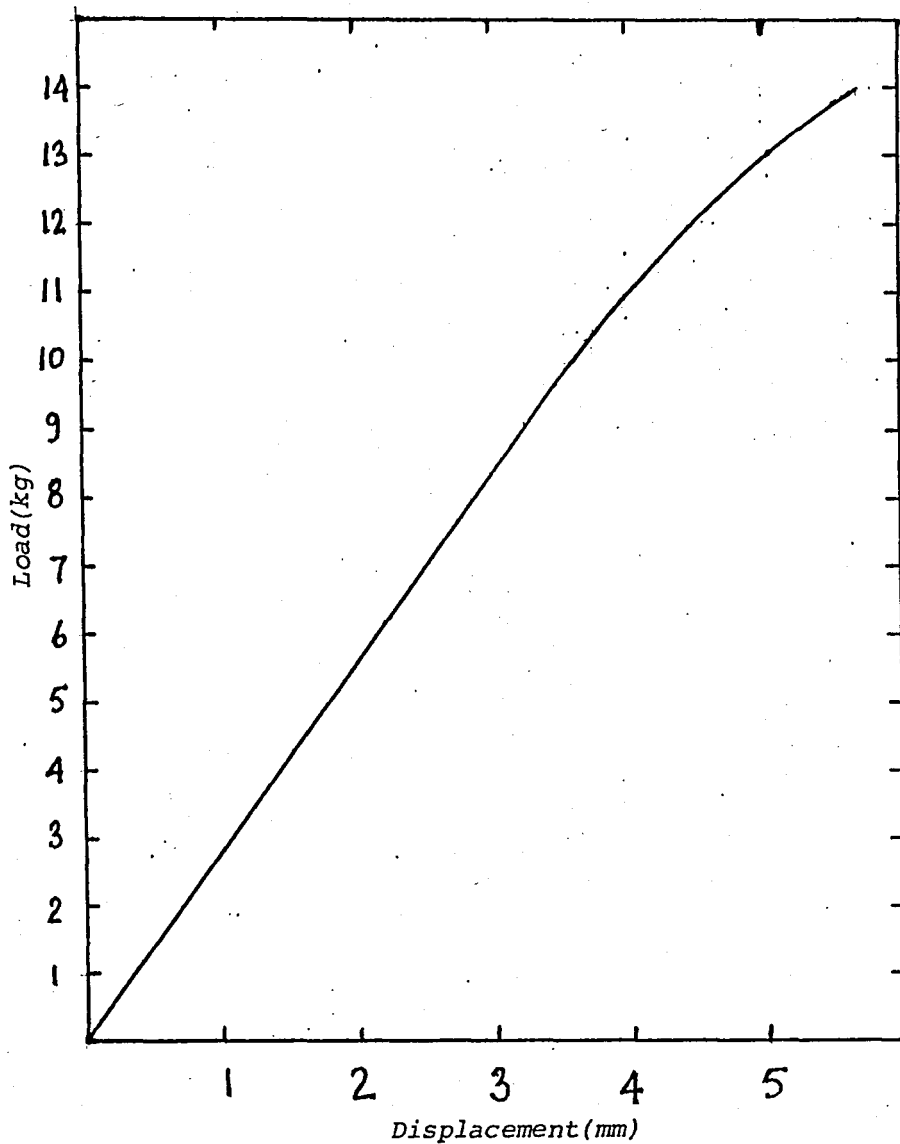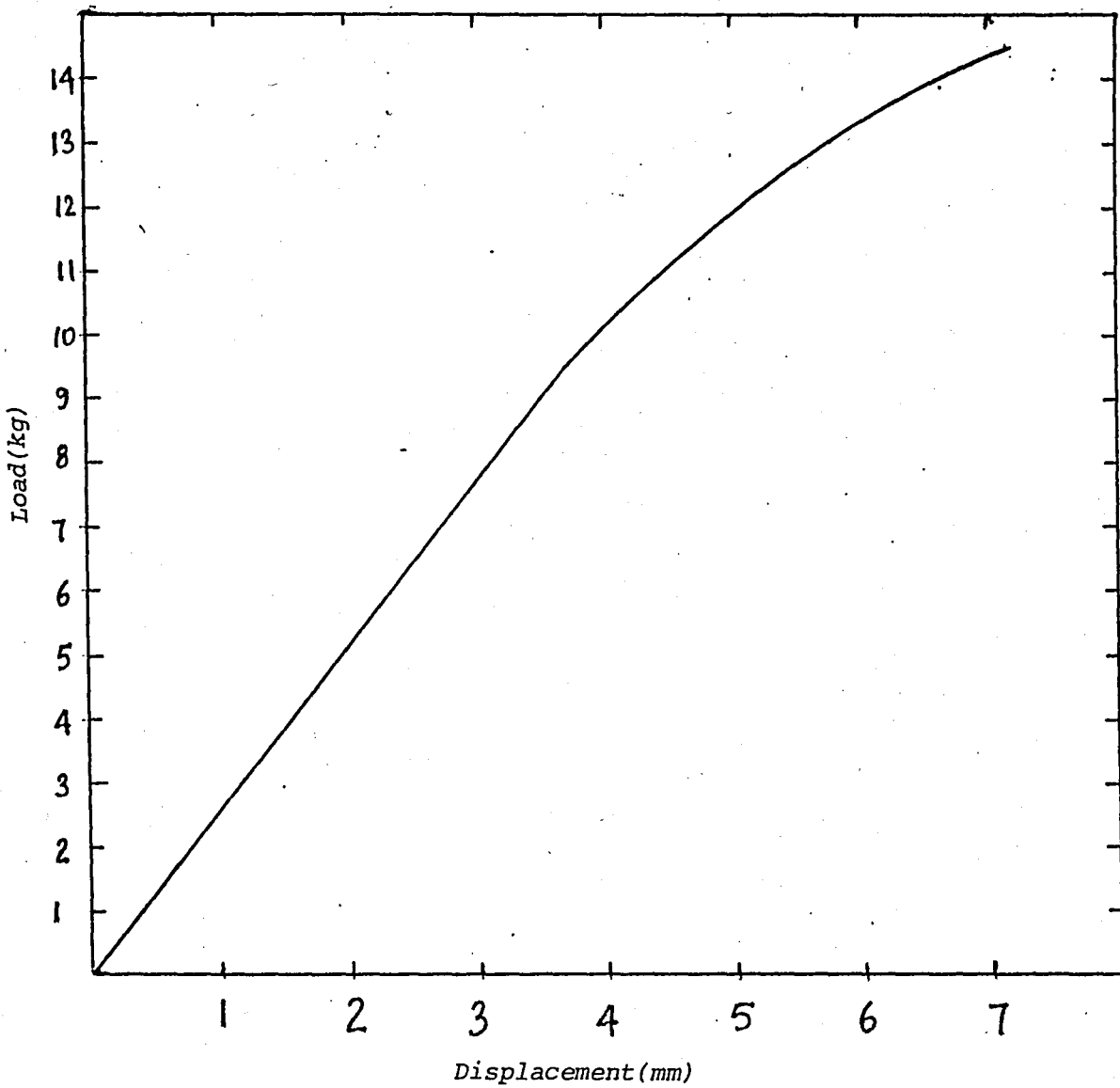FIGURE A2.6 Re-Plotted Load vs. Displacement curve for spec.14

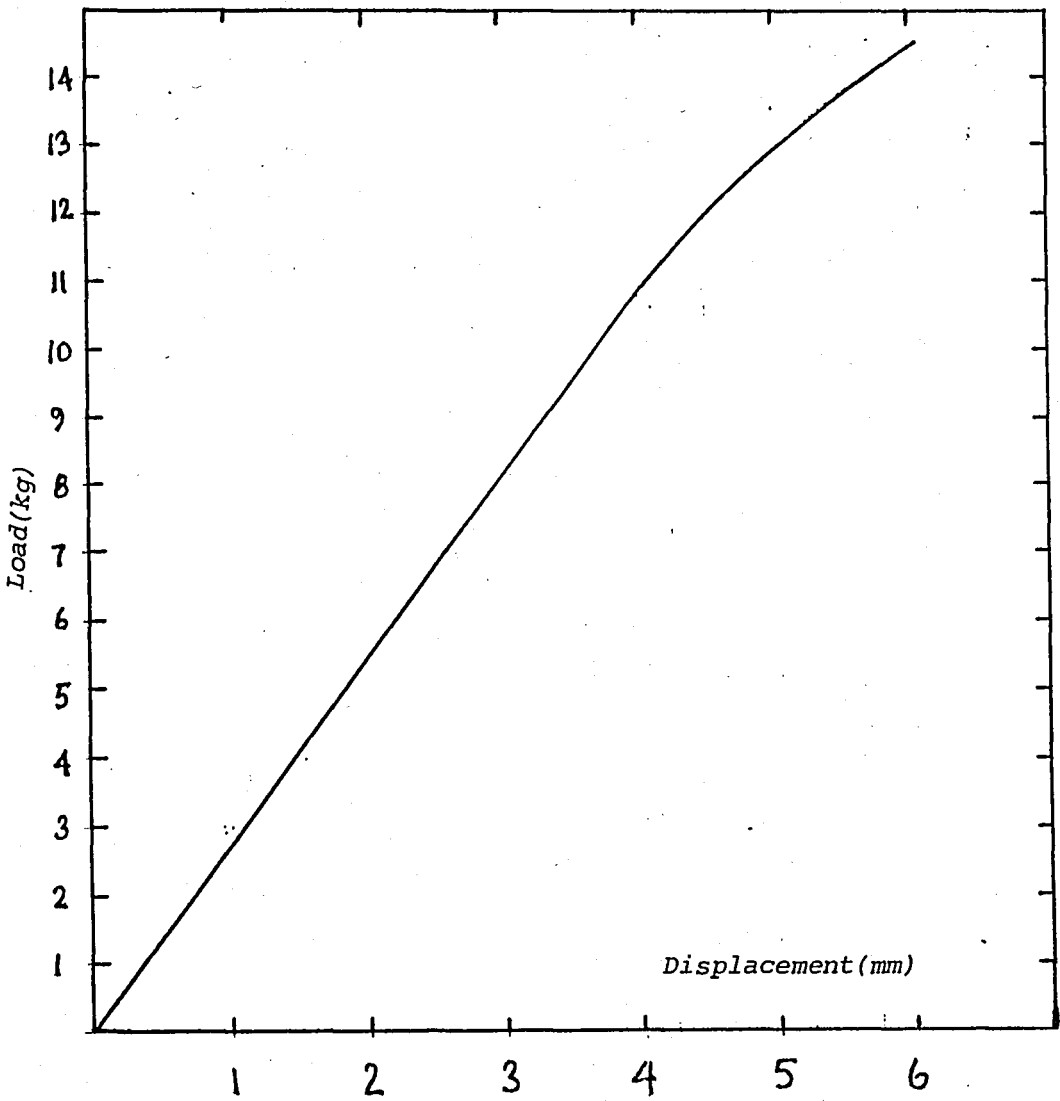FIGURE A2.7 Re-Plotted Load vs.Displacement curve for spec.15

FIGURE A2.8 Re-Plotted Load vs.Displacement curve for spec.19

# REFERENCES

1.  SMITH,E., "Predicting Stress Corrosion Crack Growth Rates When Linear Elastic Fracture Mechanics Conditions Are Not Operative", International Journal of Fracture,Vol.23,pp. 213-218,1983.

2.  SMITH,E., "Predicting Stress Corrosion Crack Growth Rates at High Stress Levels", Materials Science and Engineering, Vol.55, pp.97-104,1982.

3.  CARTER,C.S., "Application of Fracture Mechanics to Stress Corrosion Cracking", AGARD-AG-257, "Practical Applications of Fracture Mechanics", May,1980

4.  LOGAN,H.L. The Stress Corrosion of Metals. New York : John Wiley and Sons,Inc., 1966

5.  Garud,Y.S., and Gerber,T.L., "An Engineering Model For Predicting Stress Corrosion Cracking ", Int.Conference on Advances in Life Prediction Methods,pp.75-83, April 1983.

6.  VERMILYEA,D.A., DIEGLE,R.B., "Concerning Strain-Enhanced Corrosion Mechanisms of SCC ", Corrosion, Vol.32,No.1, pp.26-29, 1976

7.  HERBSLEB,G., SCHWENK,W., "The Influence of Dynamic Mechanical Parameters on Stress Corrosion Cracking of Steel-A Review", Corrosion, Vol.41, No.8, pp.431-437, 1985.

8.  ROLFE, S.T.BARSOM,J.M. Fracture and Fatigue Control in Structures, Applications of Fracture Mechanics. New Jersey: Prentice Hall, Inc., 1977.

9.  WEI,R.P., NOVAK,S.R., WILLIAMS,D.P., "Some Important Considerations in the Development of Stress Corrosion Cracking Test Methods," Materials Research and Standards MTRSA,Vol.12,No.9, pp.25-30, 1972.

10. TRUMAN, J.E., HAIGH, P.M., "Basic Aspects of Stress Corrosion : The Role of Fracture Mechanics", Journal of the Institute of Metals, Vol. 101, pp.221-224, 1973.

11. HYATT,M.V., "Use of Precracked Specimens in Stress Corrosion Testing of High Strength Aluminum Alloys," Corrosion,Vol.26,No.11,pp.487-503,1970

12. NOVAK,S.R., "A Fracture Mechanics Study on Resistance of ASTM A36,A572, and A517 Grade F Structural Steels to Stress Corrosion Crack Growth in Salt Water," Fracture Mechanics: Fourteenth Symposium-Volume II:Testing and Applications,ASTM STP 791, J.C.Lewis and G.Sines,Eds., pp.II-415-II-444,1983.

13. VAN LEEUWEN,H.P., "The Application of Fracture Mechanics to the Growth of Creep Cracks," AGARD-R-705 1983.

14. HUTCHINSON,J.W., "Fundamentals of the Phenomenological Theory of Nonlinear Fracture Mechanics", Journal of Applied Mechanics, Vol.50, pp.1042-1051, 1983.

15. LONDES,J.D., WALKER,H., CLARKE,G.A., "Evaluation of Estimation Procedures Used in J-integral Testing", Elastic-Plastic Fracture ASTM STP 668,J.D.Landes,J.A.Begley, G.A.Clarke,Eds., pp.266-287,1979.

16. LIU,H.W., ZHUANG,T., "A Dual-Parameter Elastic-Plastic Fracture Criterion", International Journal of Fracture, pp. R87-R91,1985.

17. RITCHIE,R.O., "Why Ductile Fracture Mechanics", Journal of Engineering Materials and Technology, Vol.105,pp.1-7, 1983.

18. PARIS,P.C., "Fracture Mechanics in the Elastic Plastic Regime", Flaw Growth and Fracture,ASTM STP 631, pp.3-27, 1977.

19. ZAHOOR,A., PARIS,P.C., "Ductile Tearing Instability of a Center-Cracked Panel of an Elastic-Plastic Strain Hardening Material", Journal of Engineering Materials and Technology, Vol.103,pp.46-54,1981

20. PARIS,P.C.,TADA,H., ZAHOOR,A., ERNST,H., "The Theory of Instability of the Tearing Mode of Elastic-Plasic Crack Growth", Elastic-Plastic Fracture,ASTM STP 668, J.D.Landes, J.A.Begley,and G.A. Clarke,Eds., pp.5-36, 1979.

21. SRAWLEY,J.E., "On the Relation of J to Work Done Per Unit Uncracked Area: 'Total',or Component 'Due to Crack.'", International Journal of Fracture,Vol.12,pp.470-474,1976

22. KORU, A.S., "Incubation Time in The Stress Corrosion Cracking of a Low Carbon Steel, A Fracture Mechanics Approach Using The J-Integral Parameter", M.S.Thesis, Boğaziçi University, Dept. of Mech.Eng'g, 1983.

23. NEHROZOĞLU,A., CEYHAN,K., "An Experimental Analysis of SCC Using Fracture Mechanics Methodology ME 492 Project, Boğaziçi University, Dept. of Mech. Eng'g,July 1984.